博士学位論文

Study on Multi-DOF Spherical Actuator And Intelligent Control

Junghyun Chu

2017 年 7 月

大阪大学大学院工学研究科

知能・機能創成工学専攻

Abstract

Spherical actuators have been regarded as a new trend in robotics due to their superior performances. The spherical actuator is able to perform multi degree of freedom motions using only one actuator. Therefore, a multi-DOF device using the spherical actuator can reduce its weight and the structure can be simple.

Adaptive neuro-fuzzy inference systems (ANFIS) has the advantage of expert knowledge of the fuzzy inference system (FIS) and learning capabilities of the neural networks (NN) for control of a nonlinear system. The membership function parameters are tuned using a combination of the least squares estimation and back propagation. Therefore, a control method using ANFIS will produce more accurate results compared with other control methods.

In Chapter 1, the comparison of a multi-degree-of-freedom mechanism combining a spherical actuator and plurality of motors are conducted, and the advantage of the spherical actuator and the significance of development are shown. Previous research examples of the spherical actuator are shown. In addition, the purpose of this research, “Proposal of 3-degree-of-freedom spherical actuator using voice coil motor principle” and “Feedback control using adaptive neuro-fuzzy inference system (ANFIS) control method” are shown.

In Chapter 2, in order to achieve a large angle of the tilt motion, high tilt torque, easy control and good dynamic performance, the design flow chart is considered. A new structure is described for the spherical actuator. The structure of the proposed actuator and its operating principle are described.

In Chapter 3, explained the proposed intelligent control method (ANFIS) for feedback control of spherical actuator.

In Chapter 4, Verification of a 2-DOF spherical actuator and proposed spherical actuator using ANFIS feedback control method is described. Firstly, in order to verify the ANFIS, a prototype of 2-DOF spherical actuator is described. After that, each characteristic of the proposed spherical actuator is computed by FEM simulations. Finally, the proposed spherical actuator with ANFIS control is described.

In Chapter 5, the contents of Chapters 2 to 4 are summarized and conclusion of thesis.

Contents

Chapter 1 Introduction

1.1 Research background

Many industrial applications require multi-degree-of-freedom (multi-DOF) rotation motions to achieve various targets such as robotics, precision manufacturing, and laser tracking system. Conventionally, multi-DOF rotating motions are achieved using a separate single axis motor for each axis in series or parallel. Each 1-DOF motor is connected by gears and links. A typical example is the Puma 3-axis wrist shown in Fig. 1. 1 [1]. While a single axis motor can provide accurate motions on a single axis, combinations of these single axis motors as multi-DOF mechanisms become bulky and inefficient. In addition, this mechanism has a slow response and low positioning precision due to inevitable problems such as a large backlash, non-linear friction, and kinematic singularities in the operation range. In order to solve these problems, spherical actuators that are capable of controlled motions in multi-DOF actuators were proposed as an innovative and novel type of motors. The spherical actuators are capable of multi-DOF rotational motions within a single joint. For these last few decades, spherical actuators have been a popular research topic around the world due to its advantages of compact size, high motion precision, fast response, direct driven, non-singularity in workspace and high efficiency as shown in Fig. 1. 2 [2]. In particular, the spherical actuator should be suitable for applications in robotics such as robot wrists, elbows, eyes, and shoulders [3]; other applications include a satellite attitude control [4]; and in vehicle devices such as adaptive head lamp and side-view mirrors as shown in Fig. 1. 3.

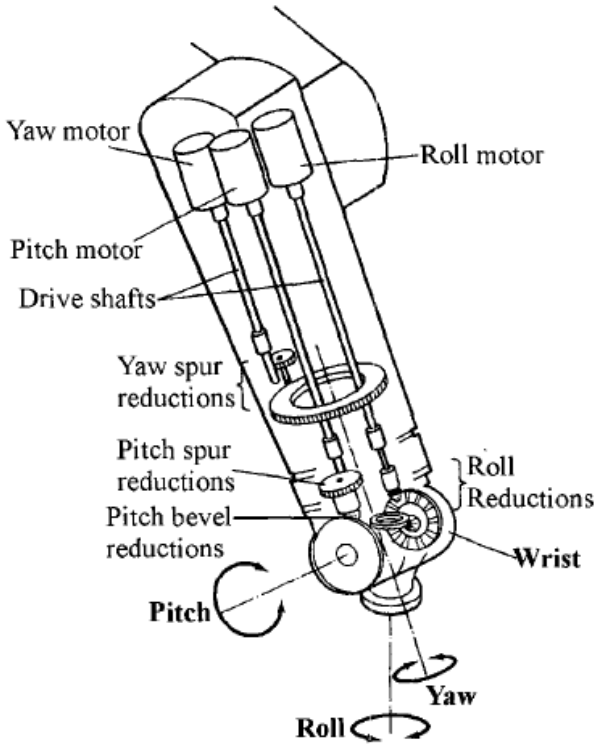

Fig. 1.1 Schematic of 3-axis wrist.

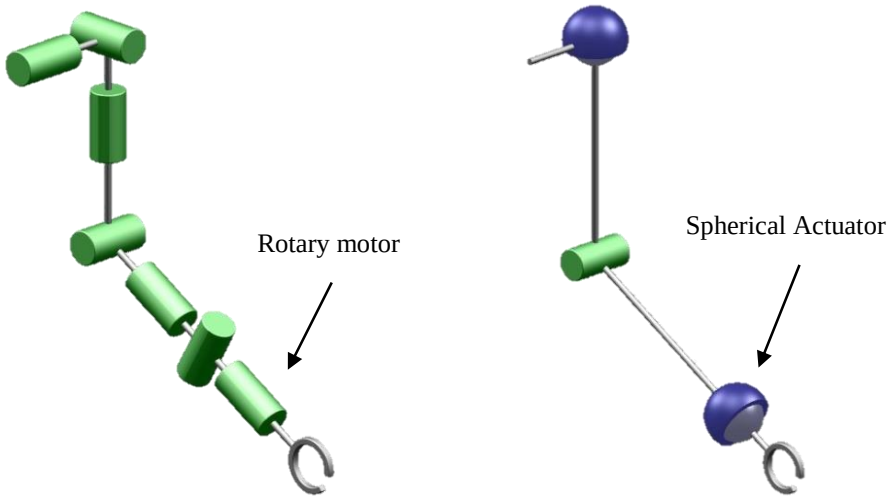

Fig. 1.2 Multi-degree of freedom driving mechanism

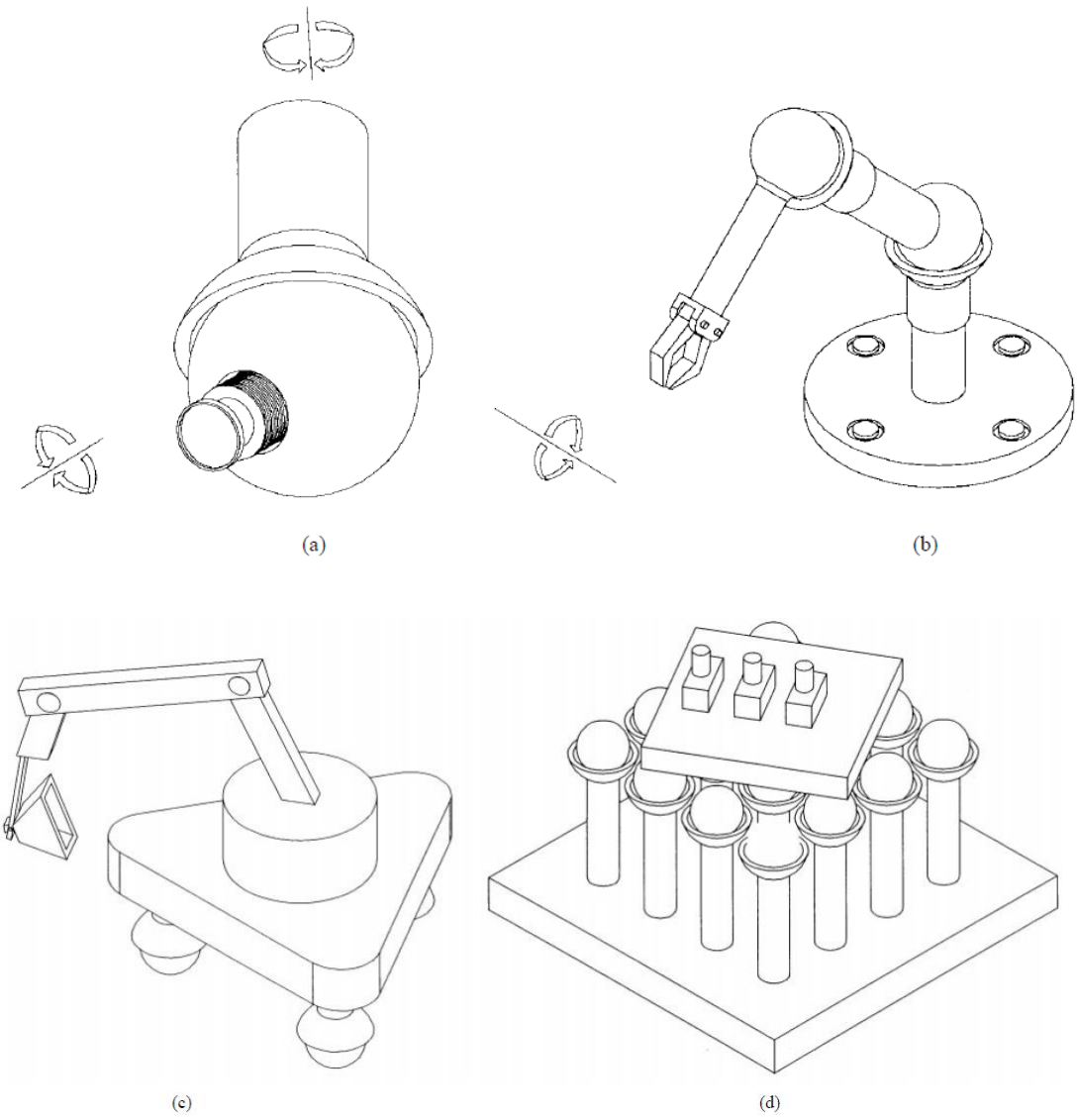

Fig. 1.3 Applications of spherical actuators [5]

1.1.1 Spherical actuator technology

Spherical actuators take a number of forms including induction motors [6-8], reluctance motors [9-15], and ultrasonic motors [16-18]. Most spherical actuators are based on the principle of electromagnetism. The three dimensional nature of the electromagnetic field distribution in almost all of the foregoing spherical actuators make their electromagnetic and dynamic behavior difficult to analyze, and this has been a significant obstacle to their design optimization and servo application. Closed-loop control systems for nonlinear electromagnetic spherical actuators especially have difficulties due to a number of uncertainties involving system identification and force/torque computation. As a result, the potential advantages of employing spherical actuators have not been realized. Therefore, most developed spherical actuators remain un-commercialized [15].

The greatest drawback associated with existing spherical actuators is that the actuating mechanism is very complicated. Most spherical actuators are based on the principle of electromagnetism. The three-dimensional nature of the electromagnetic field distribution in nearly all spherical actuators makes their electromagnetic and dynamic behavior difficult to analyze. This has been a significant obstacle which prevents the optimization of their design and their use in servo applications.

1.2 Previous researches

Multi degree of freedom spherical actuators offer the potential for much improved performance and have been the subject of research for several decades. Research into multi-DOF spherical actuators has been in progress for several decades, and various types of driving techniques have been proposed in the design of multi-DOF spherical actuators.

1.2.1 Induction spherical actuator

A spherical induction actuator was first proposed by Williams and Laithwaite et al [22]. The actuation principle of the induction spherical actuator is that the magnetic field generated by the stator windings induces a current on the rotor surface, which causes the rotor to incline. Davey proposed a general analysis of both the fields and resultant forces generic to the spherical induction actuator [6]. However, the actuator had a mechanical complexity and inherent poor servo characteristics. Dehez developed and analyzed a spherical induction actuator with magnetic teeth [8]. The stator consists of five separate inductors as shown in Fig. 2. 1. In order to minimize the air gap length and avoid friction, an aerostatic suspension of the rotor was used. The results and the topology are interesting but still, no mention of control strategies are provided to solve the low capability for a position control in the induction motor [23]. Traditionally, induction spherical actuators have not attracted commercial interests, probably due to the relatively complex stator core and winding arrangement and the inherently poor servo characteristics of induction motors.

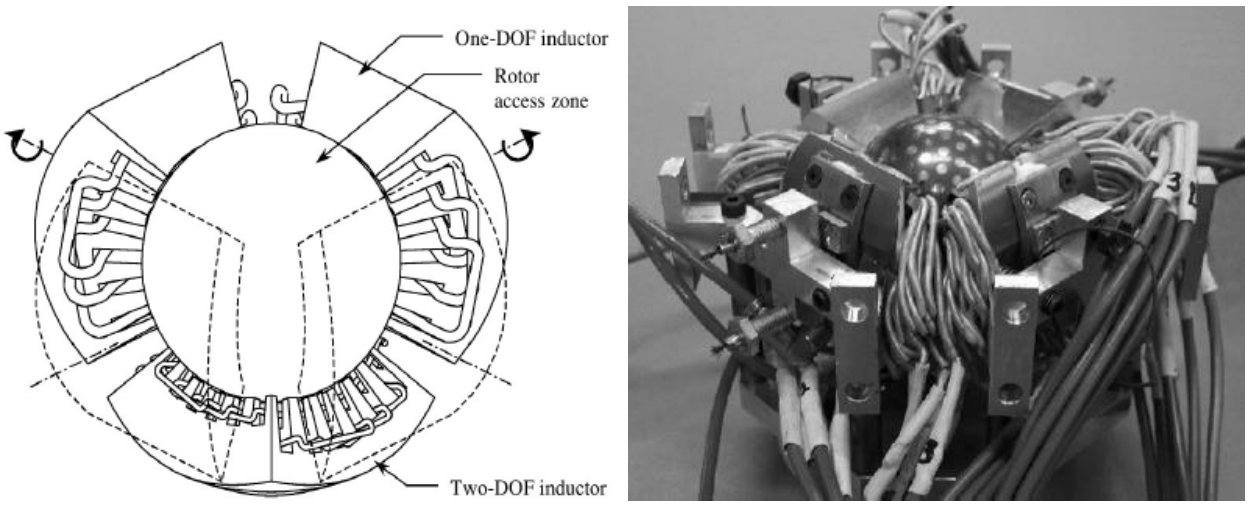

Fig. 1. 4 Induction spherical actuator [8]

1.2.2 Ultrasonic spherical actuator

The ultrasonic spherical actuator is one of the most interesting spherical actuator systems. Compared with an induction type driven by a mutual action of currents, the ultrasonic spherical actuator lacks massive windings, and its simple structure makes it lightweight and compact. The operating principle of the ultrasonic spherical actuators is a frictional drive from the elliptical motion, in which a stator generates vibration in the ultrasonic frequency range. The PZT elements are attached to the stator and can produce expansion or contraction motions after being energized positively or negatively as shown in Fig. 1. 5. The advantages of the ultrasonic actuators are its high responsiveness and compactness. Toyama has developed ultrasonic spherical actuator since 1996 [24]. He developed a novel spherical actuator which has three annular stators as shown in Fig. 1. 6 [25]. The angular velocity vector of the spherical rotor was determined by a combination of the angular velocity vector of the 3 stators. Also, a new holding mechanism using a phosphor bronze plate was developed. In cases when the output shaft is attached to the spherical rotor, the movable range is limited to approximately ±30 degrees. The ultrasonic actuator has advantages of a high motion resolution and low power consumption. The ultrasonic spherical actuators have simple and compact designs compared with other types of spherical actuators. However, it also possesses disadvantages such as low speed, complex fabrication and hysteresis. Furthermore, wear on the frictional material for long term operation may cause instability of the spherical motion.

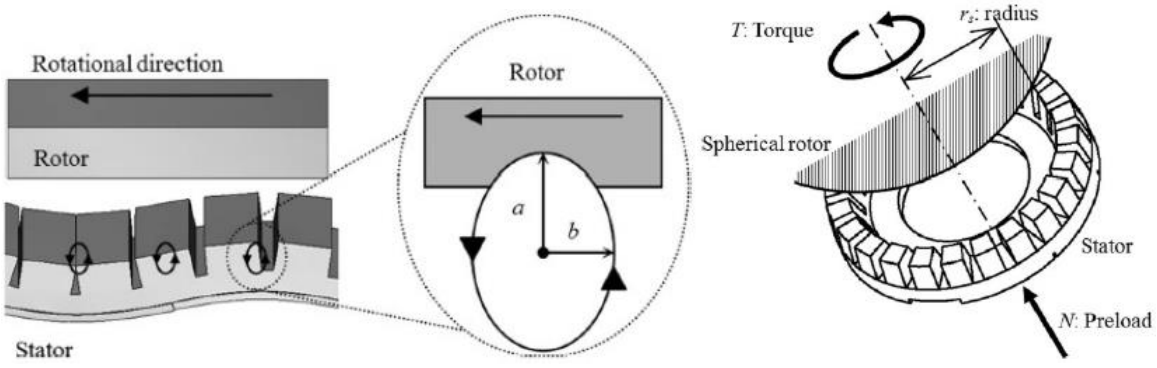

Fig. 1. 5. Elliptical motion on the surface of the stator [25]

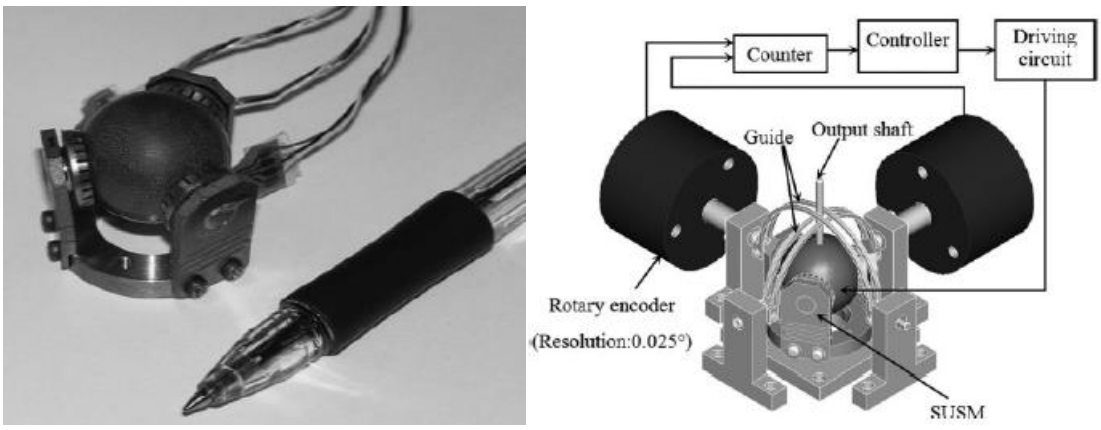

Fig. 1. 6. Novel spherical ultrasonic actuator [25]

1.2.3 Variable reluctance spherical actuator

The variable reluctance (VR) spherical actuators are the most commonly used in spherical actuator systems. The variable reluctance actuator has a relatively large movable range, possesses isotropic properties in its motion, and has relatively simple and compact designs. The operating principle of the variable reluctance spherical actuators is as follows. A permanent magnet attached along the rotor can produce a high flux density; the numerous bobbins with coils are attached to the stator. By varying the input currents of the coils, a multi-DOF rotation motion can be achieved. The reluctance spherical actuators have a relatively large movable range, high torque, and high speed. This type has been developed by Lee et al for the first time as shown in Fig. 1. 7 [9]. Generally, the variable reluctance spherical actuators consist of a globular shape stator and rotor. The stator poles are wound by coils and each coil is excited individually as shown in Fig. 1. 7 (c). This pole is symmetrically distributed on the stator surface. The rotor is made of a permanent magnet. Both the stator and rotor are a circular shape. The torque of the variable reluctance spherical actuator depends on the current inputs as well as the magnetic reluctance of the air gaps between the rotor and the stator poles. The variable reluctance spherical actuator also uses an outside gimbal guide and rotary encoder. Wang developed a novel spherical permanent magnet actuator using a similar principle [26, 27]. The spherical permanent magnet

rotor is housed within the spherical stator on a low friction surface coating as shown in Fig. 1. 8. In this type actuator, due to manufacturing tolerances both the rotor and the stator housing are not perfect spheres. This results in a significant amount of non-uniformly distributed stick-slip friction torque. For upgrading the system performance, the alternative bearing system is needed.

Variable reluctance spherical actuators are the most widely developed in multi-DOF spherical actuators. However, the control systems of the reluctance spherical actuators are very difficult to develop due to their non-linear rotor dynamics, intricate magnetic fields, and challenging measurement problems. In addition the variable reluctance spherical actuators have a relatively low specific torque capability due to the large air gap length. In attempts to solve these problems, Georgia Institute of Technology and Sheffield University have undertaken numerous studies on the torque model and control algorithm [1, 28-32]; they developed various improved spherical actuators. However the developed spherical actuators have not attracted significant commercial interest. Furthermore, the current challenges of the spherical actuators include obtaining a uniform high torque constant at various tilt angles, a wide working tilt angle, high precision positioning, sensing and control methods, rotor support methods and industrial or commercial uses.

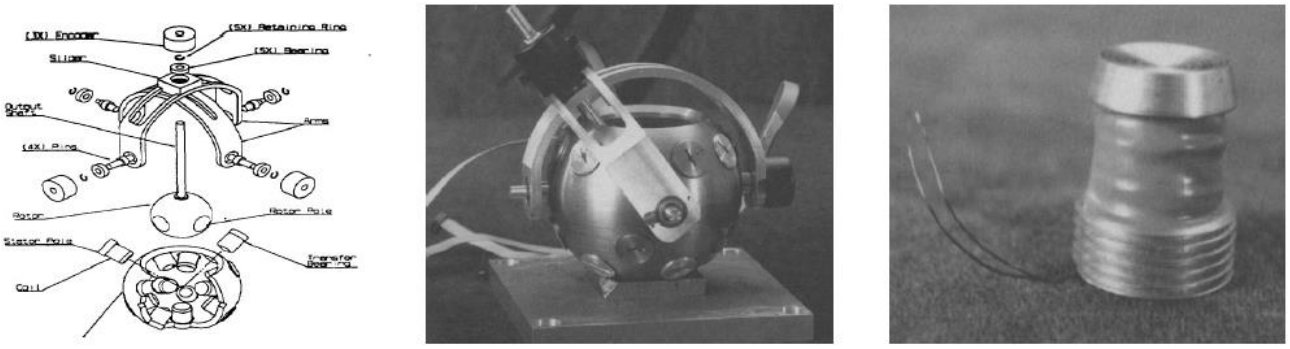

(a) Explode assembly view (b) VR spherical actuator (c) Stator pole

Fig. 1. 7 Variable reluctance spherical actuator of Lee [9]

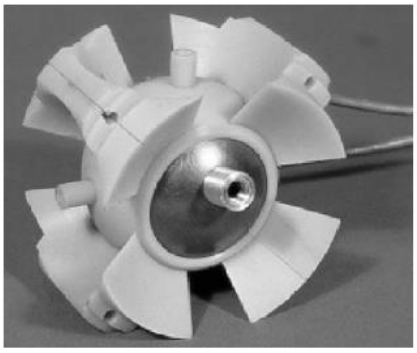

(a) rotor in stator housing

(b) stator coils

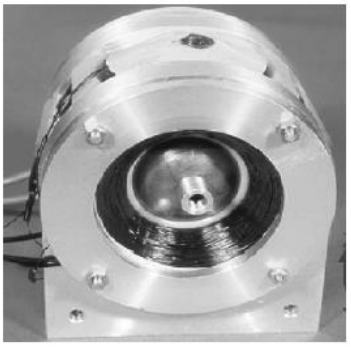

(c) spherical actuator

Fig. 1. 8 Variable reluctance spherical actuator of Wang [27]

1.3 Objective of research

1.3.1 Requirements of spherical actuator and feedback control

The requirements of spherical actuator are compact size, wide angle and the feedback control is required for more accuracy about desired value.

In this thesis, the application of proposed spherical actuator is wrist of robot. For applying the wrist of robot, the size of actuator is smaller is better, because the small size actuator can help to make compact mechanism and then if the spherical actuator can move wide angle, the mechanism of used this actuator is able to work easily. Therefore the large movable range of spherical actuator is better than other actuator.

Conventionally, the feedback control is used for more accuracy about desired value. The Proportional, Integral, and Differential (PID) control is widely used in feedback control. But the PID control uses fixed gains for calculating an error value. The fixed gains have to be obtained through many experiments so perfect gain tuning is very difficult and the using fixed gain could not adaptive sudden disturbance, but the adaptive neuro fuzzy inference system (ANFIS) control always can re-fix the gains using learning algorithm. This is one of the great advantages of ANFIS control is

automating gain tuning.

1.3.2 Objective

A main objective of this thesis is to control a multi-DOF spherical actuator using intelligent control method. The used intelligent control method in this thesis is ANFIS. The multi-DOF spherical actuator is to propose, design a novel type of spherical actuators in an application with a multi-DOF joint. The proposed spherical actuator is capable of providing the three-DOF motions required for robotic wrists.

The aim of these control strategies is to obtain improved performances in terms of disturbance rejection or parameter variation than obtained using conventional algorithms. Because of integrate the best features of fuzzy logic and neural network. Fuzzy logic control introduces a good tool to deal with complicated, non-linear and ill-defined systems. Neural network has the powerful capability for learning, adaptation, robustness and rapidity.

The key feature of the proposed spherical actuator is that it uses the same operating principle with a VCM. Owing to the simple operating principle of the VCM, the proposed spherical actuator has also a simple driving principle. The structure of VCM principle is simpler than other synchronous motor principle. Therefore the structure of proposed spherical actuator is more compact than previous spherical actuator.

1.3.3 Scope

This thesis mainly focuses on the intelligent control and the design of a novel spherical actuator. The main points to consider in this thesis are as follows.

1. Intelligent control of the proposed spherical actuator

The proposed spherical actuator is controlled by an intelligent control. The final output motion of the spherical actuator has coupled with 3-DOF rotational motions.

However, the three torque generation parts of the spherical actuator are totally decoupled. Therefore, a control algorithm which enables input currents to decouple is needed. The three degrees-of-freedom control method based on the system modeling is described.

2. Proposal of a new spherical actuator

A novel spherical actuator is proposed. The operating principle of the new proposed spherical actuator is based on a physics principle called the Lorentz force. It is easier to control compared with previously used principles of actuating.

3. Modeling and analysis of the proposed spherical actuator

Firstly, in order to calculate the forces and torques acting on the rotor, the magnetic flux distribution of the permanent magnet will be calculated at the air gap boundaries. Secondly, forces and torques will be calculated by the Lorentz force principle. Thirdly, the model will be verified using FEM tools. The verified analytical model will be used for an optimal design process.

4. Design optimization of the proposed spherical actuator

Since the performance of the spherical actuator is heavily influenced by the design parameters, an optimization procedure should be performed to obtain the best design parameters. The dimensions of the permanent magnets, coils and steel yokes are determined using design optimization frameworks in order to achieve a higher force and torque.

1.4 Concept of the proposed spherical actuator

The proposed spherical actuator aims to overcome drawbacks of existing development spherical actuators. The spherical actuators which were developed in the

past have complex manufacturing processes and non-linear rotor dynamics. Because of these drawbacks, most of the developed spherical actuators are useless in industrial applications. Therefore, my primary plan is to make a spherical actuator which is useful in industrial application first. In addition, the proposed spherical actuator should as much as possible have better performance than other spherical actuators. It is impossible to solve the above problems using conventional actuation principles (induction, ultrasonic, variable reluctance). Therefore, the actuating method should be changed. The new actuating method will be able to solve the above problems. The new concept was created based on the ideas of VCMs (Voice Coil Motor). Originally, a voice coil is a coil of wires attached to the apex of a loudspeaker cone. It provides the motive force to the cone by the reaction of a magnetic field to the current passing through it. The term is also used for similar actuators, commonly used as the positioning actuator in the disk read-and write head of computer hard disk drives as shown in Fig. 1. 9. The VCM is a kind of linear DC motors where the carriage reciprocates by the force induced by the interaction of the coil current and the magnetic flux generated by the permanent magnets in the air gap. The VCM has a simple driving principle and the constant torque coefficient characteristics. Therefore, the proposed spherical actuator uses the VCM principle. Basically, the VCM principle uses the Lorentz force principle. In physics, the Lorentz force is a force on a point charge due to electromagnetic fields. Simply, A charged particle q moving with velocity $\mathbf{v}$ in the presence of an electric field $\mathbf{E}$ and a magnetic field $\mathbf{B}$. The entire electromagnetic force $\mathbf{F}$ on the charged particle is called the Lorentz force and is given by :

$$\mathbf{F} = q\mathbf{E} + q\mathbf{v} \times \mathbf{B} \qquad (1.\ 1)$$

If the effective coil volume and external magnetic flux density are constant, the Lorentz force depends on only current. As a result, the torque is increased proportionally to the DC current input. Using these strengths of the VCM, a novel spherical actuator would be designed.

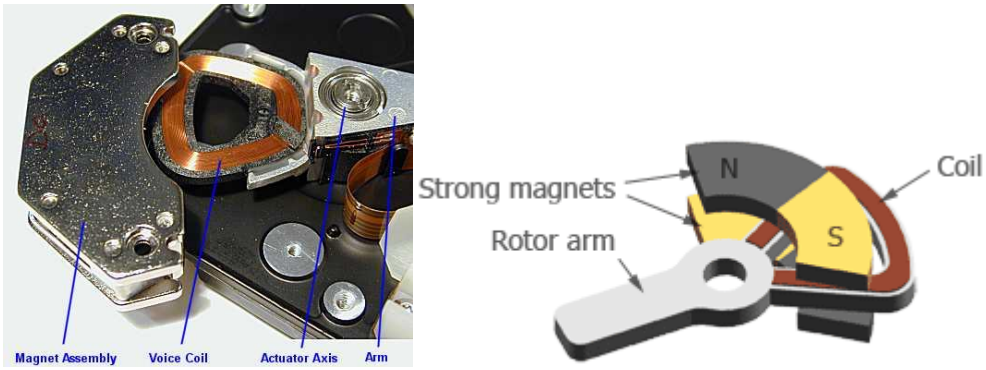

Fig. 1. 9 HDD VCM

Chapter 2 Spherical Actuator

2.1 Structure of actuator

2.1.1 Features of the proposed spherical actuator

Spherical actuators that have been developed in the past have complex manufacturing processes and non-linear rotor dynamics. As a result of these drawbacks, most of the developed spherical actuators are not useful in industrial applications. Therefore, the first aim of the proposed spherical actuator is to be useful in industrial applications. In addition, the proposed spherical actuator is designed to have better performance than existing spherical actuators. For practical applications, there is one significant design feature of the proposed spherical actuator: the moving principle. The moving principle of the proposed spherical actuator was created based on the ideas of the Voice Coil Motor (VCM). The VCM has a simple moving principle and a constant torque coefficient characteristic. Using these strengths of the VCM, the proposed spherical actuator can obtain uniform high torque, high resolution, and high accuracy.

2.1.2 Design flow chart

In order to achieve a large angle of the tilt motion, high tilt torque, easy control and good dynamic performance, the design flow chart is considered as shown in Fig. 2. 1.

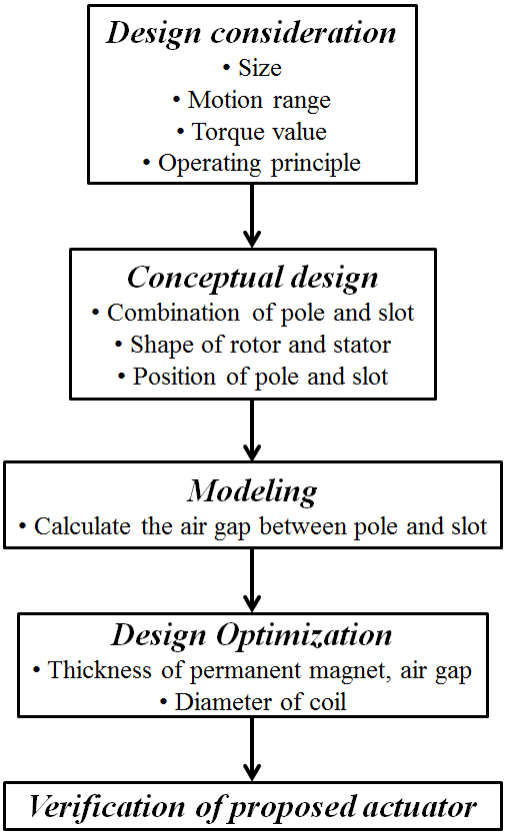

Fig. 2. 1. Design flow chart of proposed actuator

2.1.3 Design considerations

As mentioned previously, the spherical actuators have many advantages and potential applications in robotics manipulator and positioning devices. Unfortunately, most of the developed spherical actuators are useless in industrial applications. Therefore, I plan to make a new spherical actuator for uses in a real life. Several considerations for designing a new spherical actuator are summarized.

・Large working ranges

The spherical actuator will be used for applications as diverse as robotic manipulators and automated manufacturing. From the previous literature, the working range of the spherical actuators is from ±5 degrees to ±30 degrees. The working range is different depending on the application. The proposed spherical

actuator will be applied to a wrist of a robot arm. Because the wrist of the robot arm has an inherent angle of grapping, the working range of the proposed spherical actuator is designed to be ±40 degrees. Considering that the existing spherical actuator which has a ±40 working range did not have a constant torque constant at whole tilt ranges. This working range specification is of the highest levels in the development of the spherical actuators.

- Compact size

The size of the actuator is one of the main design considerations. In my case, the outside diameter is 80 mm. In general, a bigger actuator has a higher torque. The proposed spherical actuator has a small size compared to the other spherical actuators.

- High torque density

As mentioned earlier, the maximum torque does not mean anything. It is natural that the bigger actuator has a higher torque. The torque density is more important than the maximum torque. If the small actuator generates high torques, it is the best one. The torque density of the proposed spherical actuator is 0.2 Nm/A. These values were determined considering performances of literatures. Also it is large enough for my applications.

- Constant torque in whole working range

Theoretically, the proposed spherical actuator has a constant torque in whole working ranges. The most of the existing developed spherical actuators use a variable-reluctance type. The variable-reluctance actuator makes only attraction forces by inductions. The variable reluctance (VR) type actuator has nonlinear forces to current and air gap length. However, the proposed spherical actuator uses a VCM principle. The Lorentz force is independent of the rotor position if the magnetic flux density is uniform.

• Manufacturing cost

The manufacturing cost is also an important design consideration. Considering the manufacturing sizes of permanent magnets, coils and yokes, some components are designed as discrete bodies. That should not affect the performance of the actuator. I have tried to reduce the cost with an efficient design.

2.1.4 Conceptual design

The proposed spherical actuator consists of inner rotor, outer rotor and motion guide as shown in Fig. 2. 2. The outer rotor and outer stator are used for tilt motions around the X- and Y-axes.

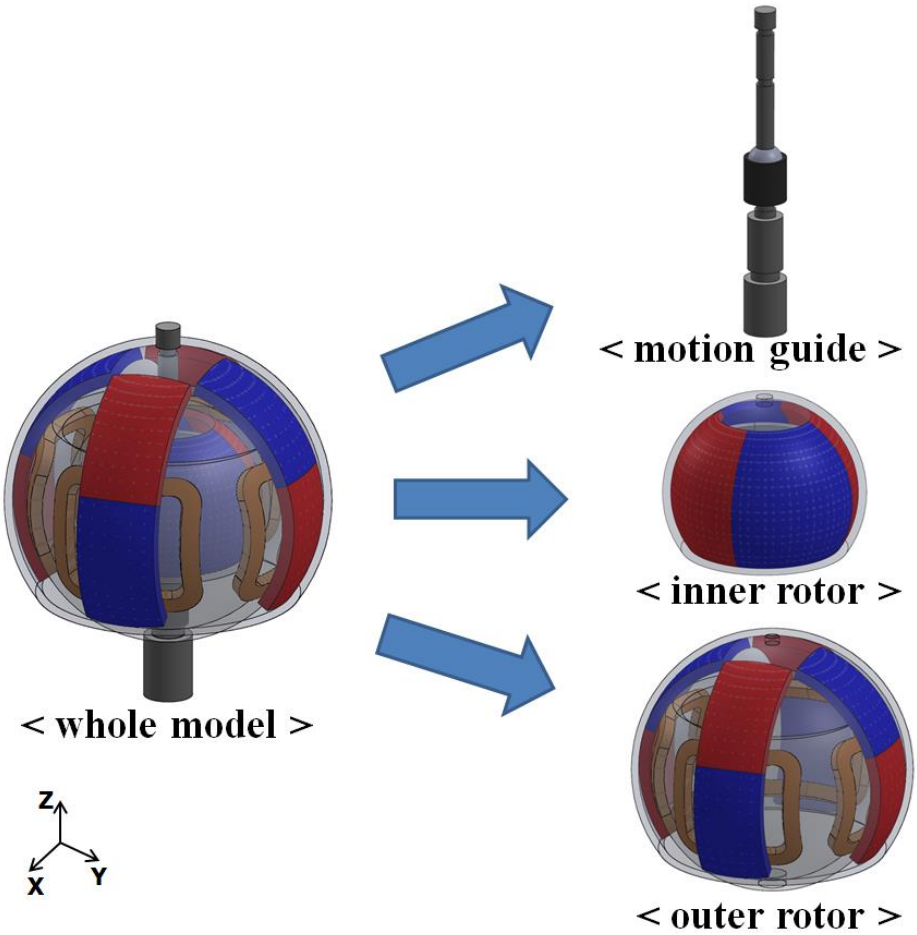

Fig. 2. 2. Schematic diagram of whole model

The outer rotor consists of 8-pole permanent magnets and 4 coils embedded into the stator as shown in Fig. 2. 3. The inner rotor and inner stator are used for a rotation around the Z-axis, which is an output shaft. The inner rotor consists of 4-pole permanent magnets and 6 coils around the Z-axis as shown in Fig. 2. 4.

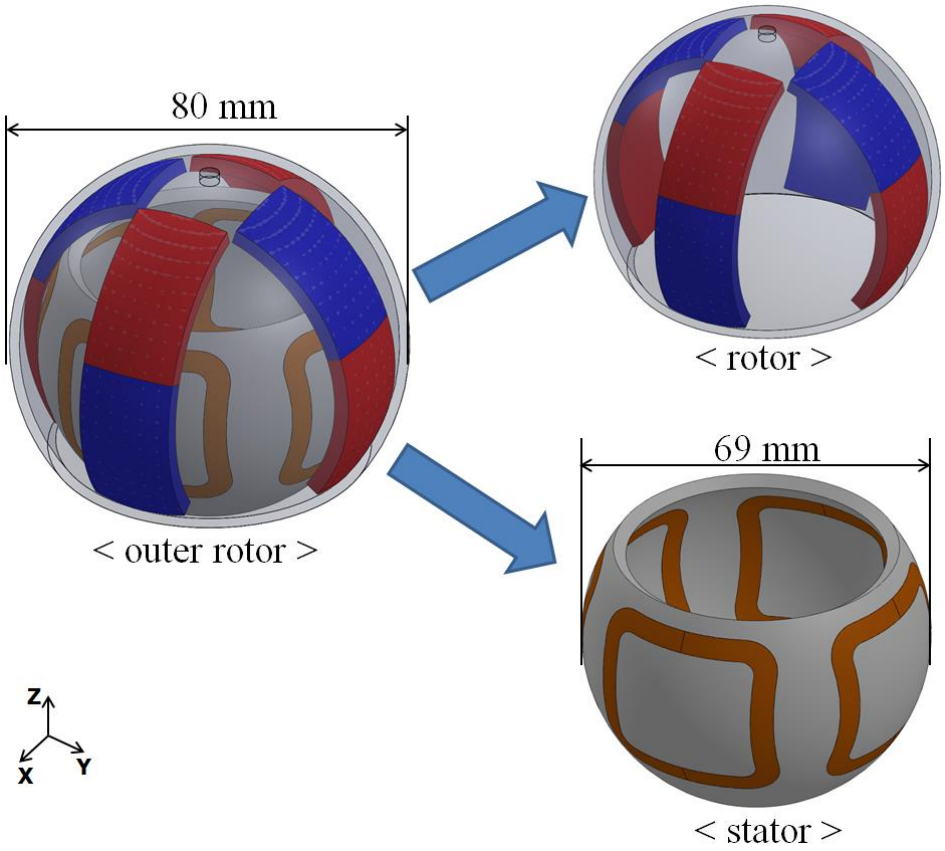

Fig. 2. 3. Schematic diagram of outer rotor

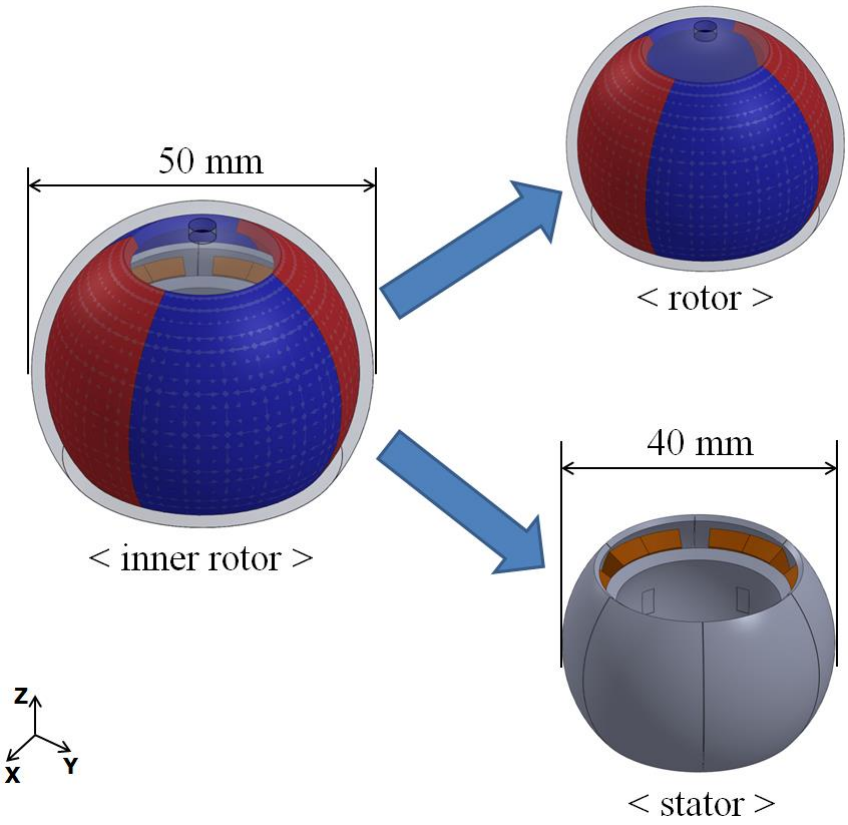

Fig. 2. 4. Schematic diagram of inner rotor

By using the motion guide, each rotor is fixed in the same axis and each stator is fixed with each other to maintain the constant air-gap length. The motion guide consists of a spherical bearing. A ball plunger is also used for maintaining the constant air-gap length. Fig. 2. 5 shows the spherical bearing and ball plunger.

(a) spherical bearing

(b) ball plunger

Fig. 2. 5. Spherical bearing and ball plunger of motion guide.

This actuator has enough space between the outer rotor permanent magnet (PM) and inner rotor PM in order to decrease the acting force of each PM. The material of the stator of the outer rotor is plastic as shown in Fig. 2. 6.

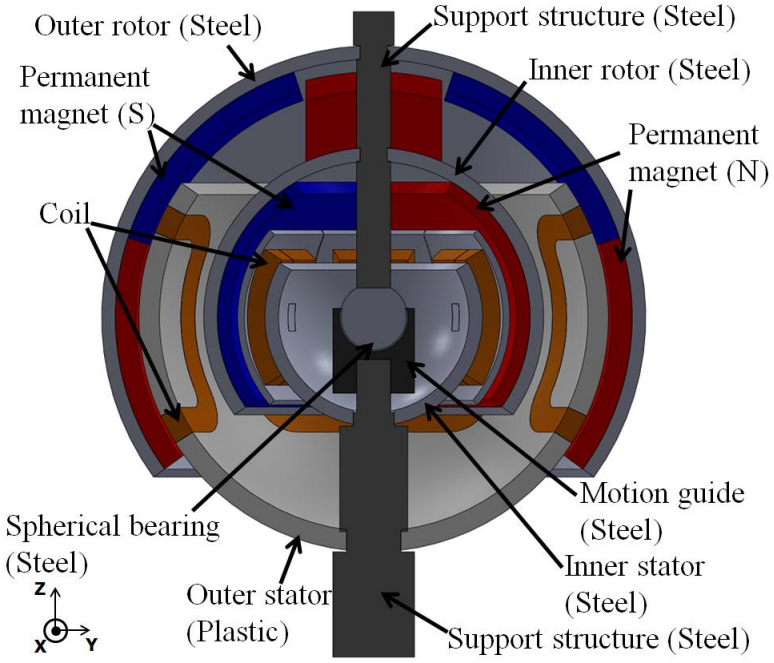

Fig. 2. 6. Y-Z cross section

2.1.5 Modeling

The analysis of the magnetic field distribution at the air gap is a prerequisite for force and torque calculations of the VCM spherical actuator. The air-gap magnetic field is a determinant quantity to predict VCM spherical actuator performances. In order to optimize the actuator performance, an analytical model of the magnetic field in the air gap must be established. Naturally, the magnetic field distribution and optimization can be calculated accurately using the 3-D FEM simulation program.

In order to optimize the proposed spherical actuator, an FEM model must be established as seen in Fig. 2. 7. The proposed spherical actuator uses a permanent magnet. The bias magnets are used to provide a prescribed field distribution over a given region. The proposed spherical actuator uses four spherical shaped permanent

magnets of the outer rotor and four spherical shaped permanent magnets of the inner rotor as seen in Fig. 2. 6.

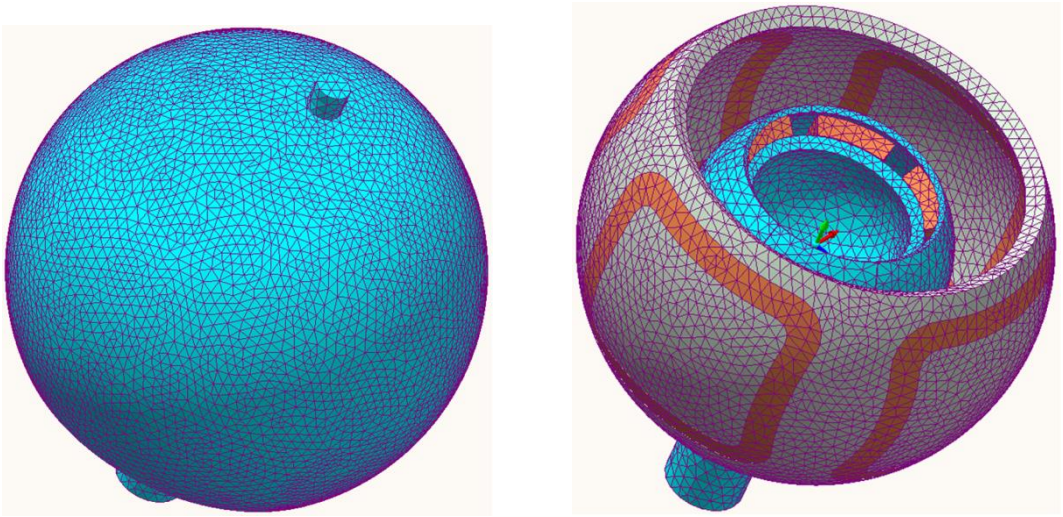

Fig. 2. 7. FEM model of proposed spherical actuator

2.1.6 Design optimization

Before the design optimization, the performance of the proposed spherical actuator should be defined. There have been numerous spherical actuators developed that have a variety of specifications. Considering the specifications of the existing spherical actuators, the performance requirements of the proposed spherical actuator are listed in Table 2. 1. The proposed spherical actuator is designed to improve the torque efficiency and precision performance compared with the existing spherical actuators.

Table 2. 1. Design specification of the proposed spherical actuator

Target specification	Quantity
Outermost diameter	80 mm
Tilt angle	± 40 degree
Torque coefficient	over 0.2 Nm/A

There are many parameters which affect the performance of the actuator. If it is

taking all these parameters into consideration, the optimal design process would be very complicated and ineffective. Therefore, some parameters are fixed as constant values.

Fig. 2. 8 shows the fixed parameters of the rotor. The yokes have enough thickness not to affect the yoke saturation. In other words, even though the design magnet has a maximum dimension value, the outer yoke does not reach a magnetic saturation state. The outermost diameter is shown in Table 2. 1. The parameters that are related to the size and working range are defined as fixed parameters. The angle between r_0 and r_1 of the permanent magnet is decided by tilt angles of the rotor. Fig. 2. 9 shows the fixed parameters of the coil. The angle of the outer stator is also decided by tilt angles of the outer rotor. The air gap length between the rotor and stator is fixed at 0.5 mm.

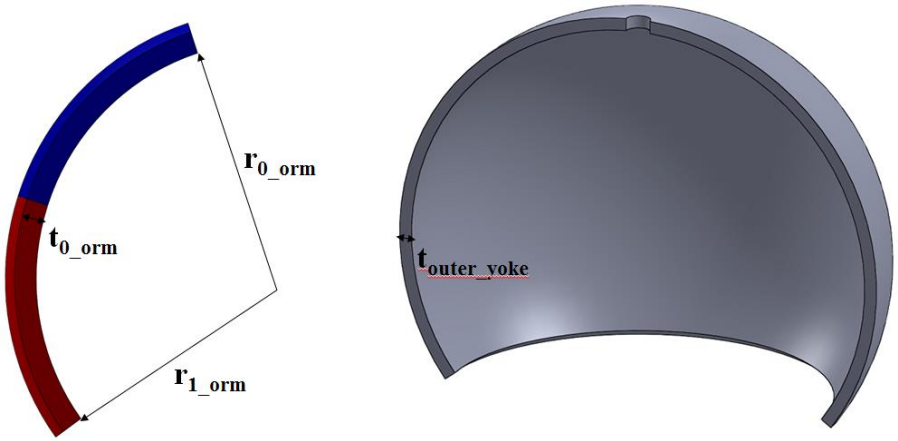

Fig. 2. 8. Fixed parameter of outer rotor magnet

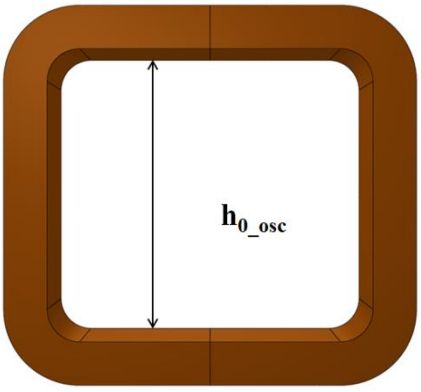

Fig. 2. 9. Fixed parameters of outer stator coil

2.1.7 Final design

Using the optimal design results, a final proposed spherical actuator is designed. The motion guide mechanism is also designed based on the system size. The actuator is fixed by a motion guide. Fig. 2. 10 presents the proposed spherical actuator. The rotor is covered with the back yoke. The final actuator's diameter is 80 mm. Table 2. 2 summarizes the final designed dimensions.

Fig. 2. 10. Final proposed spherical actuator

Table 2. 2. Final designed dimensions

Parameter		Value [mm]
Diameter	Outer rotor	80
	Outer stator	69
	Inner rotor	50
	Inner stator	40
Thickness of permanent magnet	Outer rotor	3
	Inner rotor	2

Width of permanent magnet	Outer rotor	20
	Inner rotor	24.33
Thickness of air-gap	Outer rotor ⟷ Outer stator	0.5
	Outer stator ⟷ Inner rotor	6.5
	Inner rotor ⟷ Inner stator	1
	Teeth of inner stator	0.1

2.2 Operating principle of actuator

The tilting principle around the X- and Y-axes is similar to a rotational VCM. The number of permanent magnets of each side in the outer rotor is the minimum for tilting around X- and Y-axes when using the principle of the VCM.

The proposed actuator uses one coil of each side of the outer stator for tilting around X- and Y-axes. The outer coils generate tangential directional forces that cause the tilt torques. Fig. 2. 11 shows the principle of the generation of the tilt torques. Fig. 2. 11 (a) and (b) show tilt motions from 0 to 40 degrees and (c) and (d) show tilt motions from 0 to −40 degrees.

The moving principle around the Z-axis is based on a conventional 4-pole-6-slot permanent magnet synchronous motor as shown in Fig. 2. 12. Torques when the inner rotor rotates around Z-axis are generated by a three-phase current of the inner coils. Both rotors are rotated simultaneously.

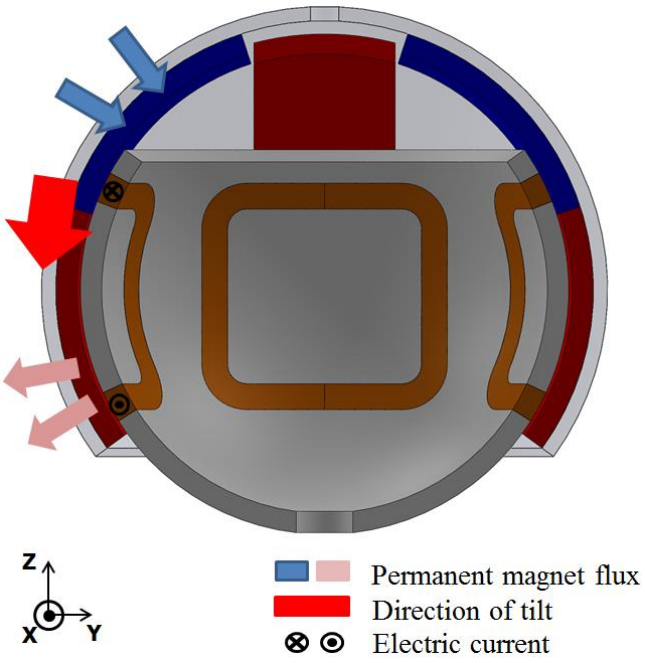

(a) Tilting motion around X-axis on 0 degree

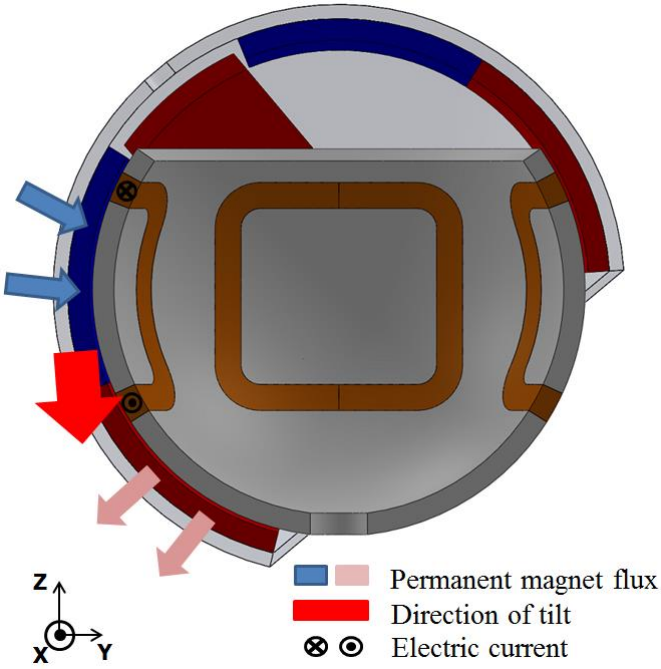

(b) Tilting motion around X-axis on 40 degree

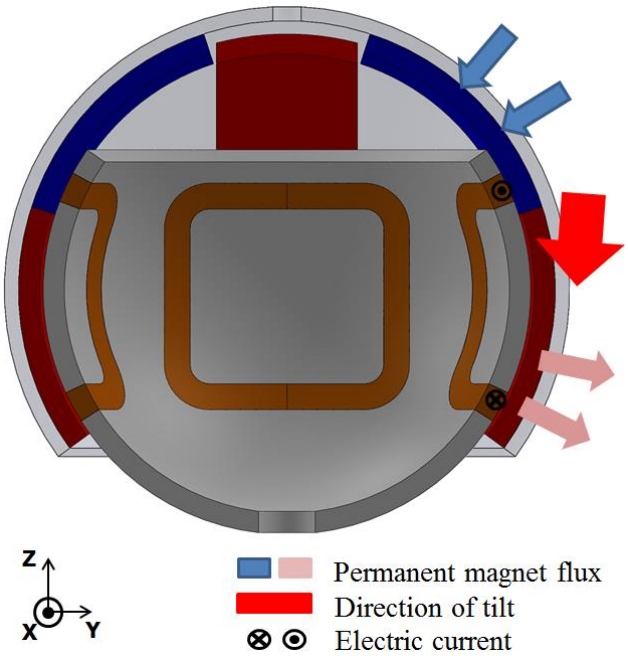

(c) Tilting motion around X-axis on 0 degree

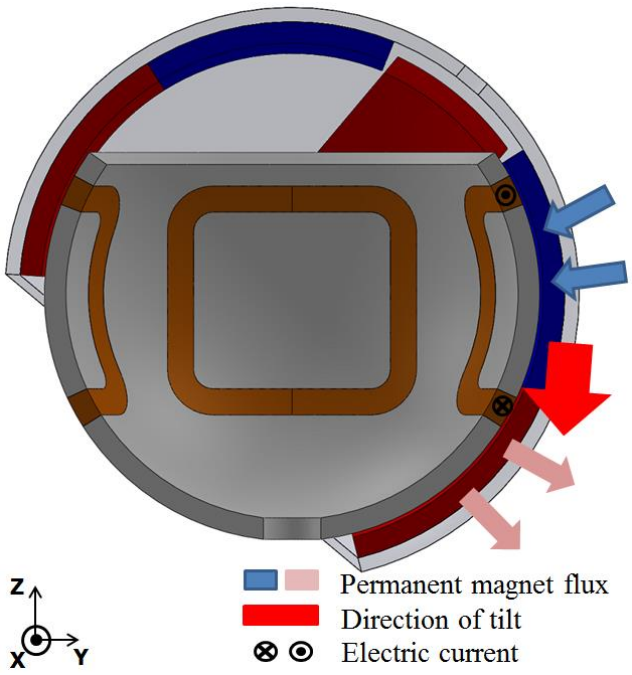

(d) Tilting motion around X-axis on -40 degree

Fig. 2. 11. Principle of generation of the tilt torque

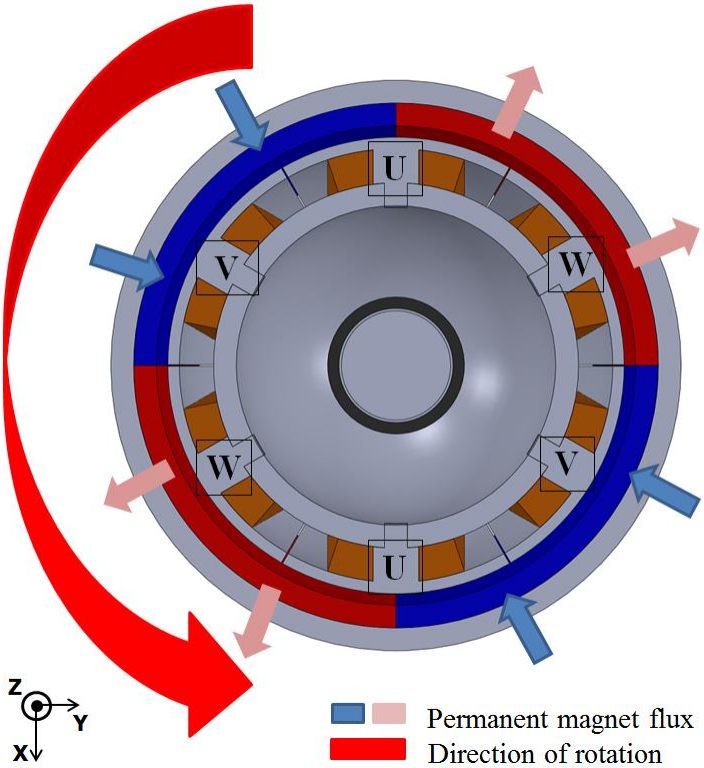

Fig. 2. 12. Rotation motion around Z-axis

Chapter 3 Intelligent Control Method

Many feedback control algorithms such as PID (Proportional, Integral, and Differential) control, fuzzy control and neural network control for actuator control have been proposed. A PID controller is a control loop feedback mechanism controller widely used in industrial control systems [33]. The PID controller calculates an error value as the difference between a measured process variable and a desired value using fixed gains which have to be obtained through many experiments, which is a disadvantage. The adaptive neuro-fuzzy inference system (ANFIS), which was developed in the early 1990s by Jang [34], combines the concepts of the fuzzy logic [35] and neural networks [36, 37, 38] to form a hybrid intelligent system that enhances the ability to automatically learn and adapt. The adaptive network is a network of nodes and directional links. These networks learn the relationship between inputs and outputs using learning rules such as a back propagation [39]. Therefore, a control method is expected to produce more accurate results compared to other control methods.

3.1 Adaptive Neuro-Fuzzy Inference System (ANFIS)

The fuzzy logic systems implement fuzzy sets to model uncertainty and approximate knowledge reasoning, but the fuzzy logic architecture lacks learning rules. The neural network systems strengthen adaptive learning rules for numerical sets to fit nonlinear data, but the neural network feature lacks knowledge representation.

The neuro-fuzzy systems include intelligent systems which combine the main

features of both the fuzzy logic and the neural network systems to solve problems that cannot be solved with desired performance by using either the fuzzy logic or the neural network methodology alone [40]. The ANFIS is a fuzzy inference system embedded in the framework of adaptive networks which provides the best optimization algorithm for finding parameters to fit the given data. Based on human reasoning in the form of fuzzy "IF-THEN" rules, the ANFIS develops the mapping of input and output data pairs using a hybrid learning procedure. The hybrid learning procedure of the ANFIS uses the backpropagation gradient descent algorithm in backward pass to tune the premise parameters of membership functions and least squared error (LSE, also known as Widrow-Hoff learning rule) [41] method in forward pass to adjust the consequent parameters of output functions.

Jang presented three types of the ANFIS [34] and I use type-3 ANFIS, which uses Takagi-Sugeno's fuzzy "IF-THEN" rules whose outputs are a linear combination of input variables and a constant.

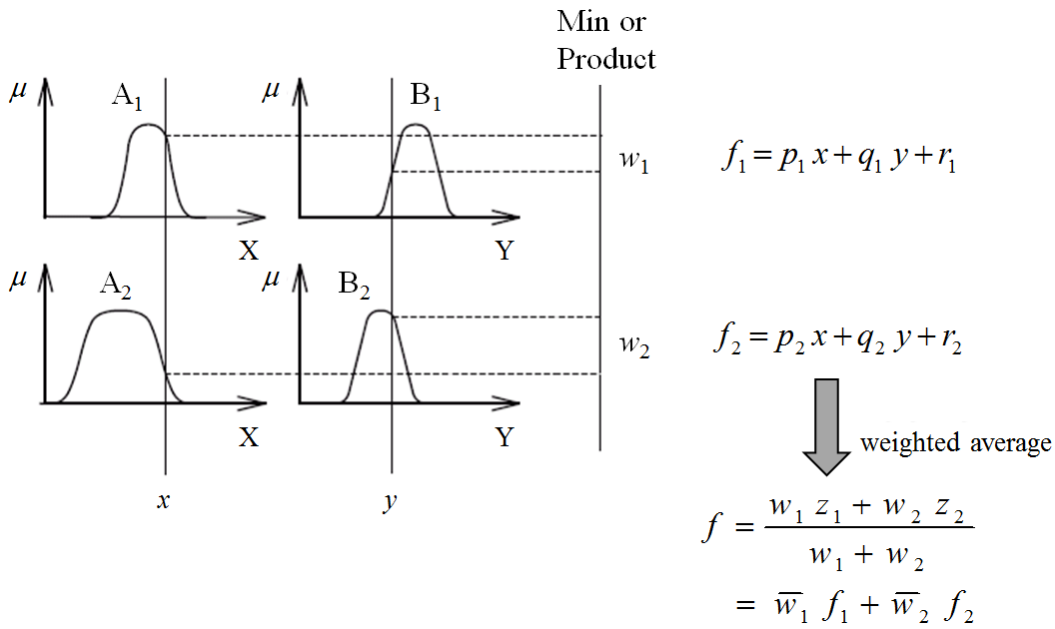

Fig. 3. 1. Two-input first-order Sugeno fuzzy model with two rules

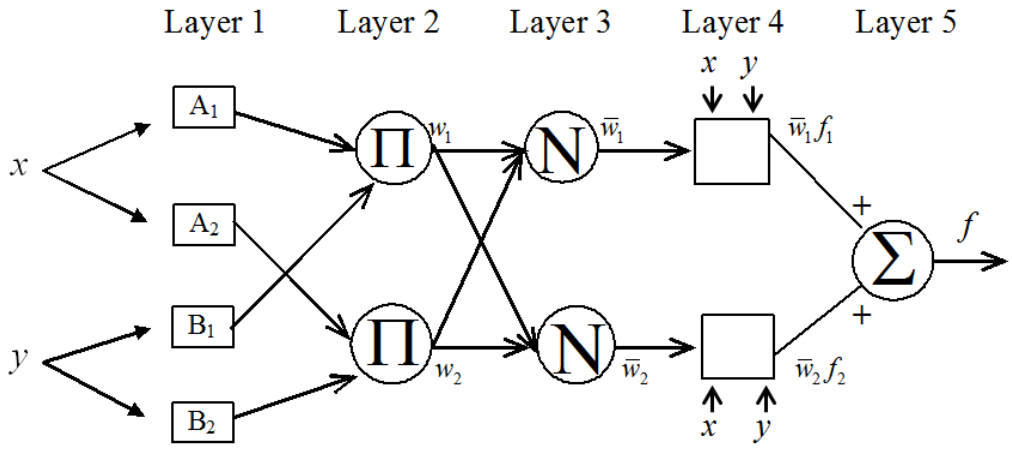

Fig. 3. 2. ANFIS architecture

To simply summarize the type-3 ANFIS architecture, I assume that x and y are two input variables and $f(x, y)$ is one output variable. As shown in Fig. 3. 1, for a first order Sugeno fuzzy model [42], a typical rule set with two fuzzy IF-THEN rules can be expressed as

Rule 1: IF (x is A_1) and (y is B_1), THEN ($f_1 = p_1x + q_1y + r_1$),

Rule 2: IF (x is A_2) and (y is B_2), THEN ($f_2 = p_2x + q_2y + r_2$).

where A_i and B_i (i = 1, 2) are the linguistic label (like *small, medium, large*, etc.) and p_i, q_i and r_i (i = 1, 2) are the linear consequent parameters.

Fig. 3. 2 depicts the corresponding equivalent of the ANFIS architecture with five layers which is composed of a fuzzification layer, product layer, normalization layer, defuzzification layer and aggregation layer.

Layer 1: fuzzification layer

I define that $O_{i,j}$ is the output of the jth node in the ith layer and square nodes (i = 1, 4) are adaptive nodes with parameters, while circle nodes (i = 2, 3, 5) are fixed nodes without parameters. Nodes j (= 1, 2) in this layer i (= 1) are square (adaptive) nodes with node functions

$$O_{1,j} = \mu_{A_j}(x) \qquad (3.\ 1)$$
$$O_{1,j} = \mu_{B_j}(y)$$

where the two crisp input x and y to nodes j are fuzzified through membership functions (1) of the linguistic labels correlated to the node functions $O_{1,j}$. The commonly used membership functions are triangular, trapezoid, Gaussian-shaped and bell-shaped membership functions.

The bell-shaped membership function can be given by

$$\mu_{A_j}(x) = \frac{1}{1+\left|\frac{x-c_j}{a_j}\right|^{2b_j}} \qquad (3.\ 2)$$

where $\{a_j,\ b_j,\ c_j\}$ is a parameter set. Parameters in this layer are referred to as premise/antecedent parameters.

Layer 2: product (T-norm operation) layer

Each node (j = 1, 2) in this layer (i = 2) is circle (fixed) node labeled product (or T-norm) operator $\prod$ with node functions $O_{2,j}$. The nodes in this layer multiply all incoming signals and send the product outputs to next layer (layer 3), which represent the firing strength of fuzzy antecedent rules ("IF" part). The outputs in this layer acts as weight functions w_j and can be expressed as

$$O_{2,j} = w_j = \mu_{A_j}(x) \otimes \mu_{B_j}(y) \qquad (3.\ 3)$$

Layer 3: normalization layer

Each node (j = 1, 2) in this layer (i = 3) is circle node labeled N with node functions $O_{3,j}$. The jth node in this layer calculates the ratio of the jth rule's firing strength to the sum of

all rules' firing strengths. The outputs in this layer normalize the weight functions that are transmitted from the previous product layer and the normalized weight functions (firing strengths) $\overline{w}_j$ can be written as

$$O_{3,j} = \overline{w}_j = \frac{w_j}{w_1 + w_2} \qquad (3.\ 4)$$

Layer 4: defuzzification (consequent) layer

Each node (j = 1, 2) in this layer (i = 4) is square nodes with node functions $O_{4,j}$. The jth node in this layer defuzzifies the fuzzy consequent rule ("THEN" part). The defuzzified outputs in this layer are multiplied by normalized firing strengths based on the formulation

$$O_{4,j} = \overline{w_j} f_j = \overline{w_j}(p_j x + q_j y + r_j) \qquad (3.\ 5)$$

where $\overline{w_j}$ is the normalized firing strength from the previous layer (third layer) and $\{p_j, q_j, r_j\}$ is a parameter set. The parameters in this layer will be referred to as consequent parameters.

Layer 5: aggregation (summation) layer

The single node in this layer (i = 5) is a fixed node labeled $\sum$ with a node function $O_{5,1}$, which computes the overall output as a summation of all incoming signals and can be expressed as

$$O_{5,1} = \sum_j \overline{w_j} f_j = \frac{\sum_j w_j f_j}{\sum_j w_j} \qquad (3.\ 6)$$

In the ANFIS architecture, there are adaptive nodes in the first layer and fourth layer. To optimize this parameter needs learning algorithm. There are two learning algorithms

developed by Jang et al. [43], namely hybrid learning algorithm and backpropagation. The hybrid learning algorithm is an algorithm that combines of two methods which is least-squares and gradient descent. There are two steps in this method, forward and the backward movements. In the forward movement, the network input will propagate forward until the fourth layer, where the consequent parameters will be identified by using a least-square method. In the backwards movement step, after calculating the error, the error signal will propagate backward and the premise parameters will be fixed by using a gradient-descent method. In this thesis, hybrid learning algorithm is selected for training the ANFIS model.

In the determining network topology of ANFIS, refer to the problem to be solved, the number of input membership function and the number of rule is determined principal component analysis with initial data. In order to determine the optimal numbers of membership function and the numbers of rule, several numbers of clustering around 2 to 3 are evaluated. After several numbers of clustering are evaluated, each model adopts an appropriate number of rules.

Chapter 4 Verification

In this chapter, the manufactured 2-DOF spherical actuator will be controlled using ANFIS and 3-DOF spherical actuator will be analyzed using ANFIS. The 3-DOF spherical actuator modeling results with the optimal design process in chapter 2 are analytically verified.

4.1 Experiments of 2-DOF spherical actuator with intelligent control

4.1.1 Basic structure of 2-DOF spherical actuator

The 2-DOF spherical actuator is composed of a stator and rotor as shown in Fig. 4. 1 and 4. 2. In the rotor, six rows of identically polarized N and S pole shell-shaped permanent magnets are arranged around the Z-axis. On the other hand, the stator has 24 teeth with 310 turn concentrated windings on each pole. They are also arrayed around the Z-axis at even intervals as shown in Fig. 4. 3. This structure makes it similar to controlling a 16-pole-12-slot synchronous motor the X- and Y-axes.

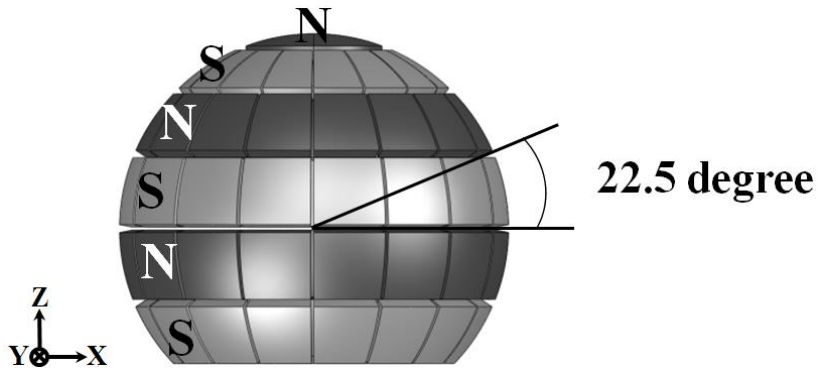

(a) Magnets arrangement of rotor

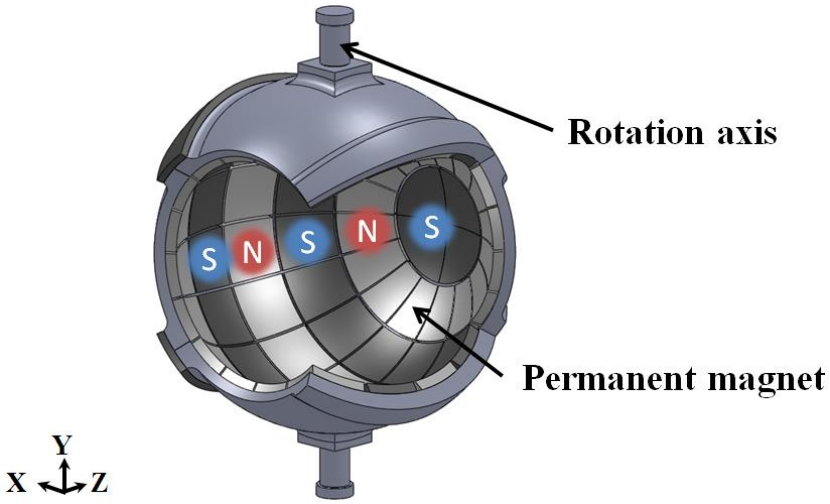

(b) Structure of rotor

Fig. 4. 1. Rotor of the 2-DOF spherical actuator

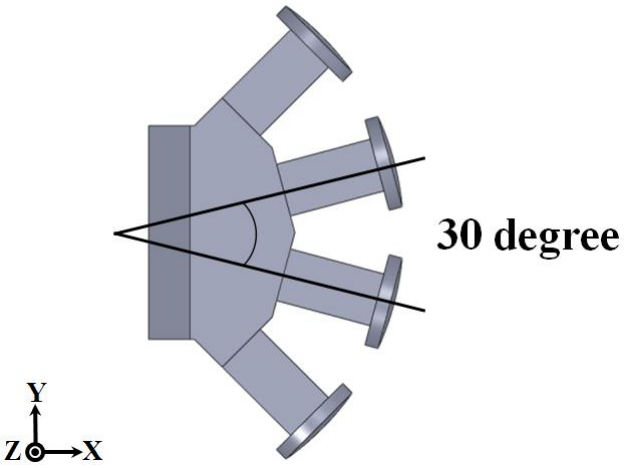

(a) Magnetic pole of stator

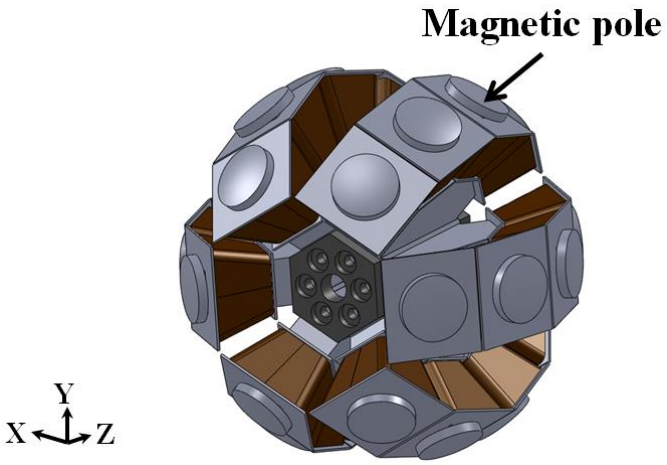

(b) Structure of magnetic poles

Fig. 4. 2. Stator of the 2-DOF spherical actuator

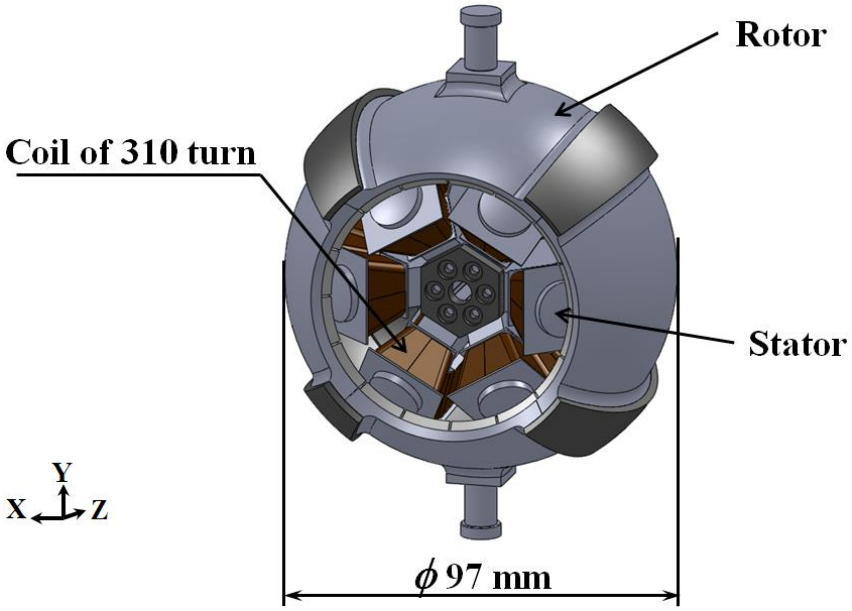

Fig.4. 3. 2-DOF spherical actuator

4.1.2 Proposed controller scheme and prototype

A schematic diagram of the experimental system using the ANFIS controller is shown in Fig. 4. 4. In this system, feedback control is conducted by ANFIS which adds a modification signal into the desired trajectory before it is input the current generator.

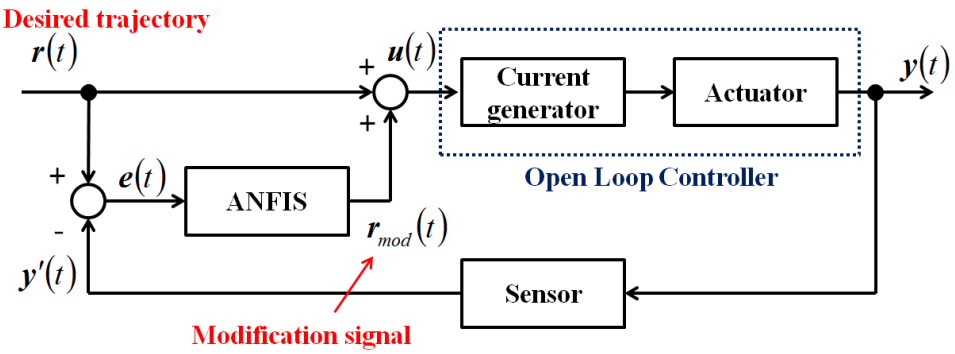

Fig. 4. 4. Block diagram of the proposed controller scheme

Current patterns of the current generator are decided by using the block diagram shown in Fig. 4. 5. When a desired signal is given as a trajectory, this system produces current patterns for all coils to track the given trajectory. The block diagram is explained below.

When a desired trajectory is given, the system calculates a current pattern for all coils as follows:

$$I_i = -\sin(8\alpha_i) \tag{4. 1}$$

where the subscript i expresses the i-th pole, I_i and A_i are the current and amplitude, respectively, and α_i is the mechanical angle between the i-th EM pole and unknown parameters A_i and α_i are derived from the following equations:

$$A_i = \frac{1}{\|\boldsymbol{k}'' \times \boldsymbol{p}_i''\|}(k'' \times \boldsymbol{p}_i'')_{x''} \tag{4. 2}$$

$$\alpha_i = \tan^{-1}\left(\frac{p_{zi}''}{\sqrt{p_{xi}''^2 + p_{yi}''^2}}\right) \tag{4. 3}$$

where $\boldsymbol{k}''$ and $\boldsymbol{P}_i''=[p_{ix}'' \; p_{iy}'' \; p_{iz}'']^T$ are unit vectors of the axis Z'' axis and position vector observed in the rotor coordinate, respectively. To calculate those two parameters, the position vector $\boldsymbol{P}_i''$ should be known and it is calculated by using the following equations:

$$\boldsymbol{p}_i = {}^{WORLD}T_{AXIS}\,{}^{AXIS}T_{ROTOR}\,\boldsymbol{p}_i'' \qquad (4.\ 4)$$

where $\boldsymbol{P}_i$ is a position vector of the i-th vector observed in the world coordinate, ${}^{WORLD}T_{AXIS}$ and ${}^{AXIS}T_{ROTOR}$ are the transformation matrixes from the world coordinate ($X\ Y\ Z$) to the axis coordinate ($X'\ Y'\ Z'$) and from the axis coordinate to the rotor coordinate($X''\ Y''\ Z''$), respectively.

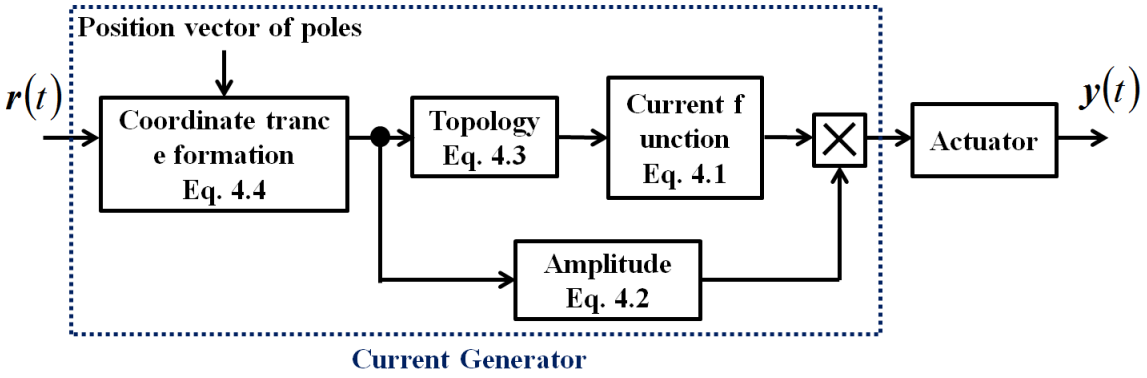

Fig. 4. 5. Block diagram of the open loop controller

A schematic of the control system using a prototype of the actuator is shown Fig. 4. 6. The prototype of the actuator used in this research is shown Fig. 4. 7. The rotor is supported by a two-DOF gimbal structure. Rotary encoders are installed in both axes of the gimbal structure, and the dynamic characteristics are measured.

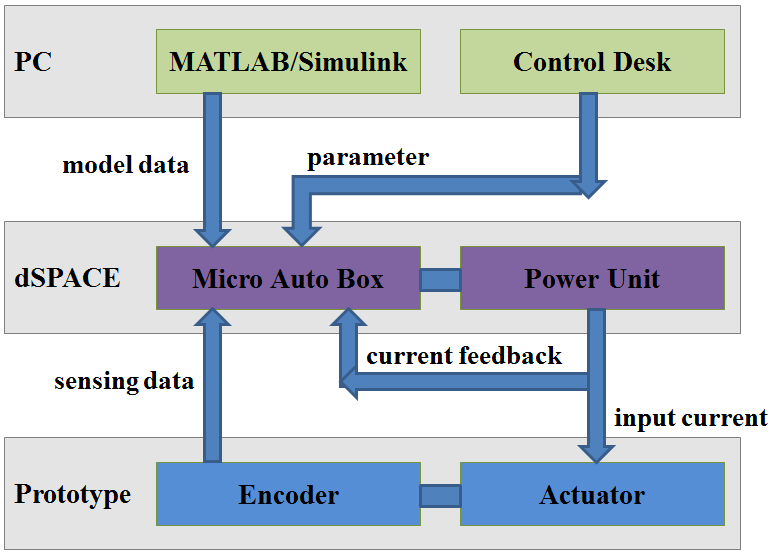

Fig. 4. 6. Schematic of the control system

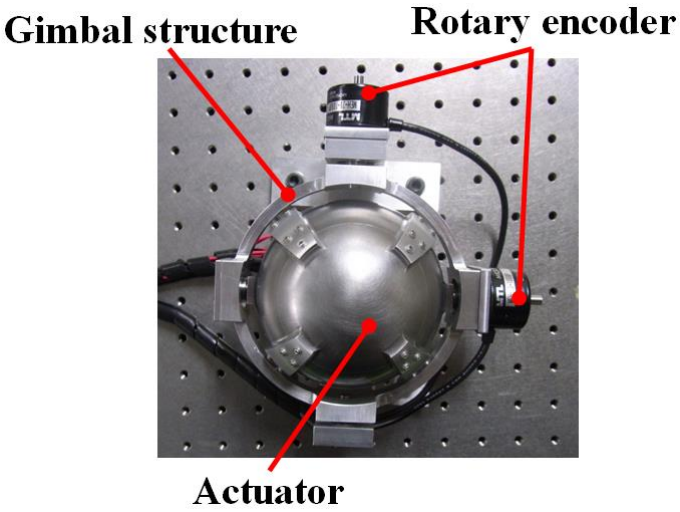

Fig. 4. 7. Prototype of the actuator

4.1.3 Experimental results

The rotation angle on the X and Y axes is ±30 degrees, as shown in Fig. 4. 8. Basically, the rotor is designed to have a ±35 degree working range. However, to prevent bumping the coil cover and the end of the yoke, the proposed spherical actuator should be tested in the safe region.

All actual rotation angles of the actuator are shown with solid lines obtained from

the two rotary encoders of the gimbal structure.

The result of the experimentation under open loop control is shown in Fig. 4. 8 and Fig. 4. 9 where both rotation angles obtained from the rotary encoder are far from the desired values. These results indicate that a control method without sensor feedback systems makes it impossible to obtain the desired values. When the actuator changes the direction, the shape of the solid line is rough because the open loop control system does not use the feedback values.

The result of the experimentation under PID control is shown in Fig. 4. 10 and 4. 11 where the position feedback system performs rather well, although small errors can be observed. The actual rotation angle of the PID control has more smooth line like the shape of the desired angle. But, the actual angles are not accurate values.

The result of the experimentation under ANFIS control is shown in Fig. 4. 12 and 4. 13 where the ANFIS control method is much more accurate and the error value between the desired and actual angles are smaller than that of an open loop control and PID control.

The average errors when open loop, PID and ANFIS controls are used are shown in Table 4. 1. The average errors of open loop, PID and ANFIS controls are about 5 degrees, about 2 degrees and about 1 degree, respectively.

As mentioned above, the ANFIS control is superior in terms of an accuracy.

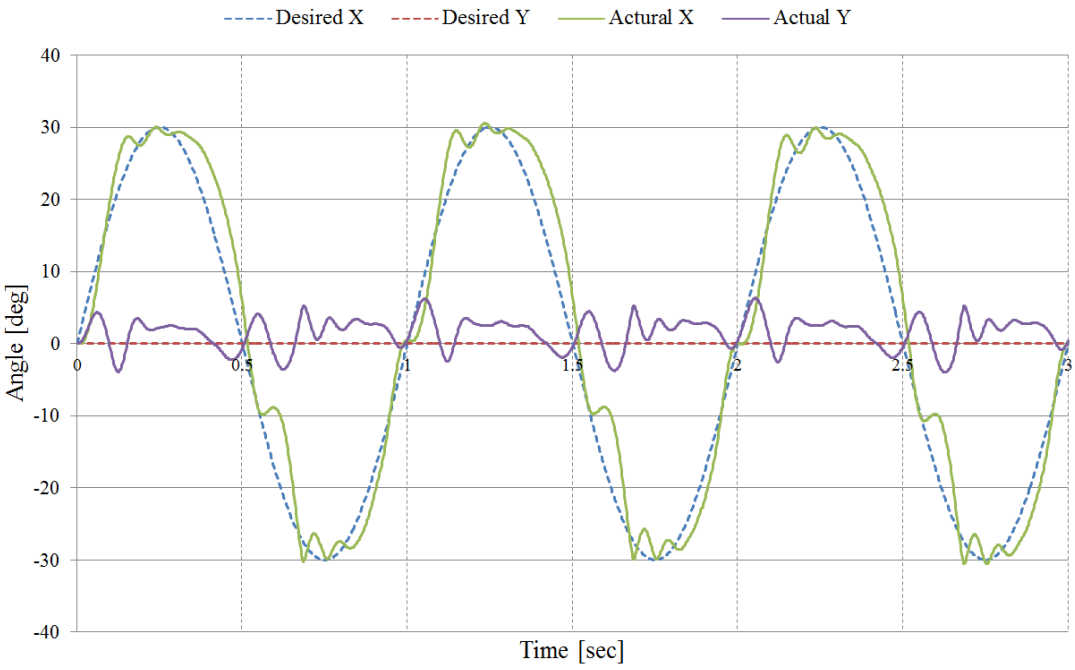

Fig.4. 8. Result of the open loop control, around X-axis

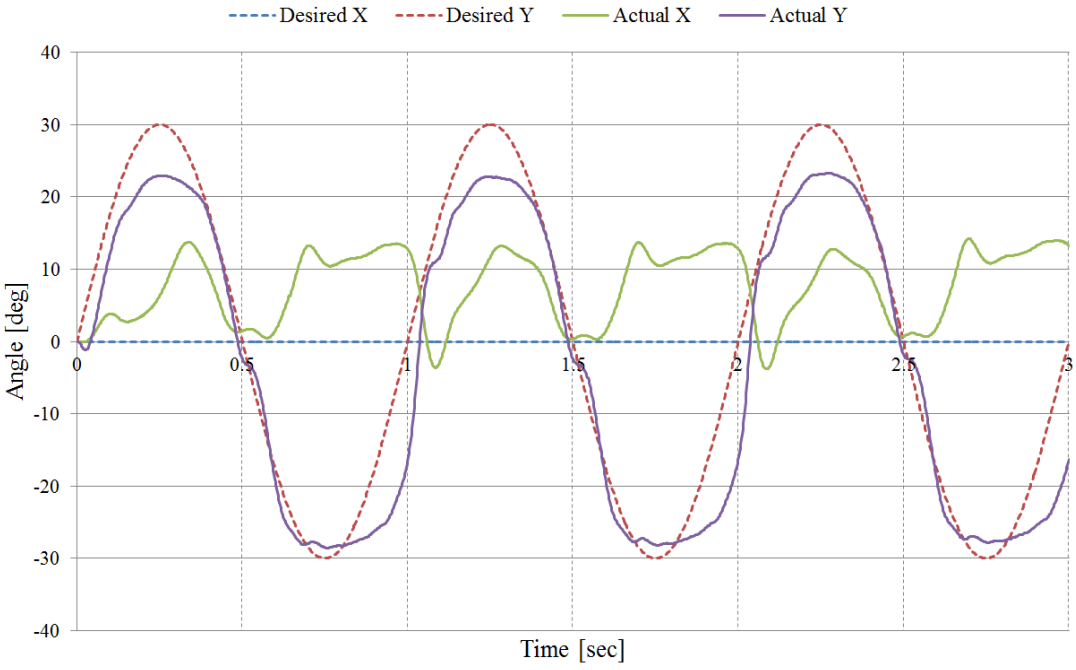

Fig.4. 9. Result of the open loop control, around Y-axis

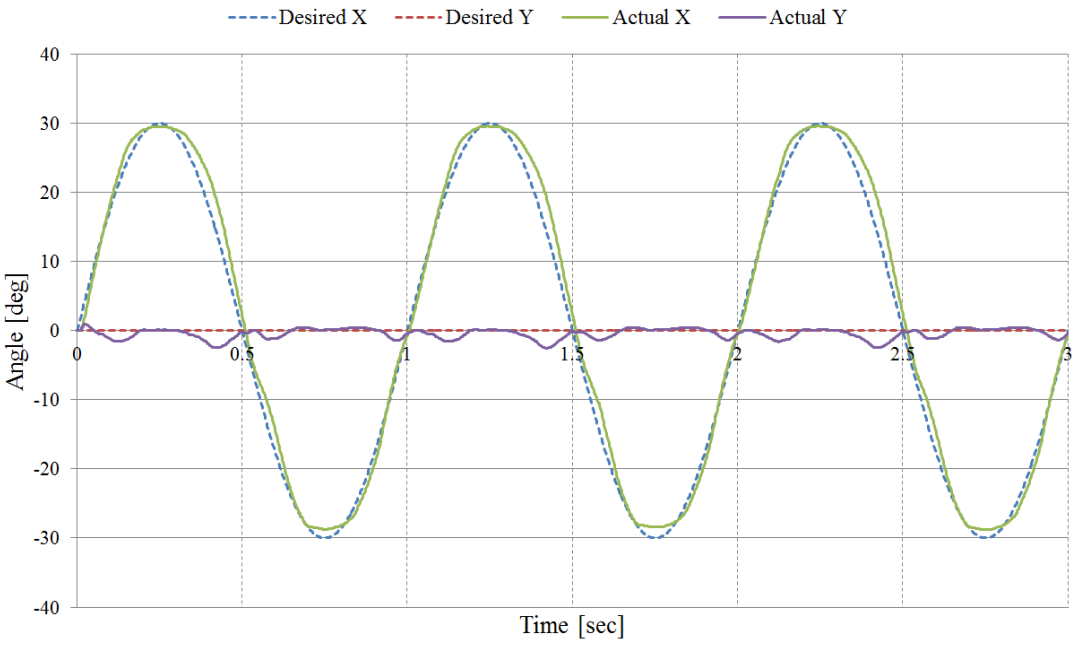

Fig.4. 10. Result of the PID control, around X-axis

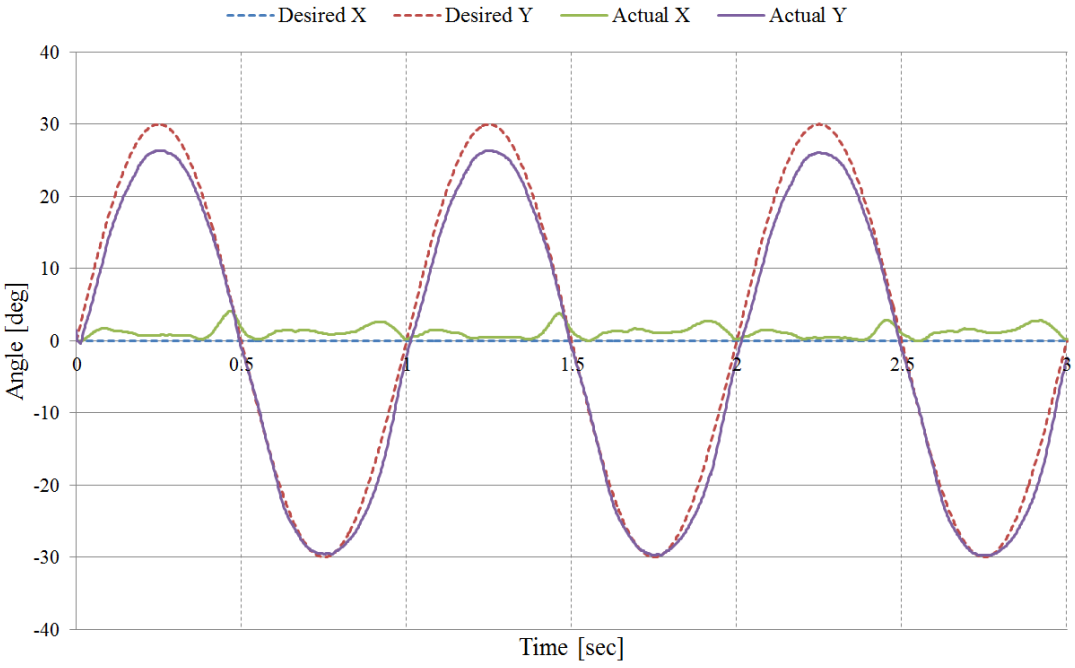

Fig.4. 11. Result of the PID control, around Y-axis

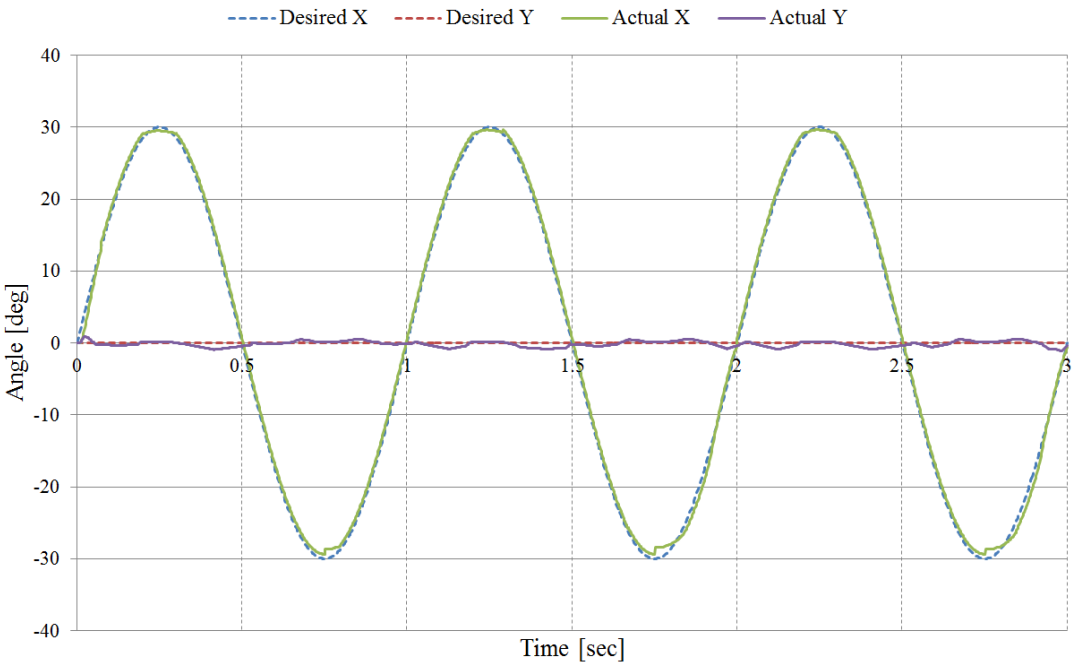

Fig.4. 12. Result of the ANFIS control, around X-axis

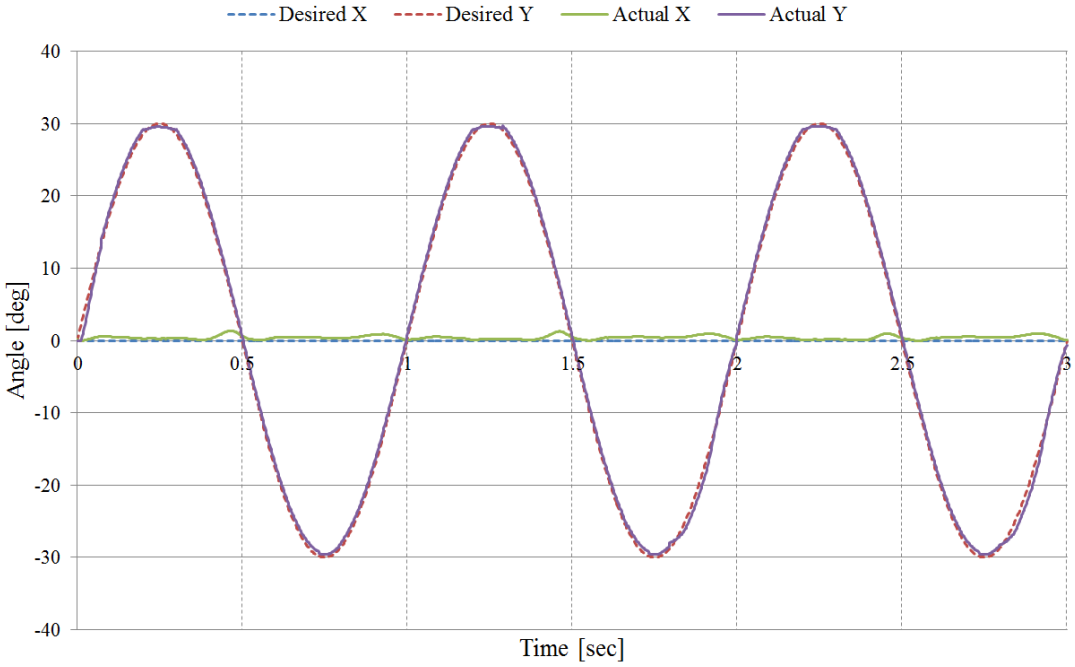

Fig.4. 13. Result of the ANFIS control, around Y-axis

Table 4. 1. Average error of each control method

Control method	Average error around X axis (degree)	Average error around Y axis (degree)
Open loop control	4.377	5.515
PID control	2.000	2.032
ANFIS control	0.740	1.036

4.2 Analyzed results of 3-DOF spherical actuator with intelligent control

4.2.1 Characteristic analysis

4.2.1.1 Analysis method

An electromagnetic field analysis using 3-D finite element method (FEM) is conducted to determine the static torque characteristics and the dynamic operating characteristics of the proposed actuator. These characteristics of the actuator are computed by employing the Ω-method given in (4. 5) through (4. 7).

$$\mathrm{div}\{\mu(\boldsymbol{T}_m + \boldsymbol{T}_0 - \mathrm{grad}\,\Omega)\} = 0 \tag{4. 5}$$

$$\left\{\begin{array}{l} \boldsymbol{J}_m = \mathrm{rot}\,\boldsymbol{T}_m \\ \boldsymbol{J}_0 = \mathrm{rot}\,\boldsymbol{T}_0 \end{array}\right\} \tag{4. 6}$$

$$\boldsymbol{H} - (\boldsymbol{T}_m + \boldsymbol{T}_0) = -\mathrm{grad}\,\Omega \tag{4. 7}$$

where μ is the permeability, $\boldsymbol{T}_0$ and $\boldsymbol{T}_m$ are the current vector potential derived fr om the forced current density $\boldsymbol{J}_0$ and equivalent magnetization current density $\boldsymbol{J}_m$, respectively, as given in (4. 6), and Ω is the magnetic scalar potential as is given b y (4. 7). $\boldsymbol{H}$ is the magnetic field intensity. Equation (4. 5) is computed by using Gale rkin's method and then the magnetic force is determined by using Maxwell's stress method. The dynamic characteristics are computed in each axis combined with the motion equation is given as follows.

$$I_i \frac{d^2\theta_i}{dt_i^2} + D_i \frac{d\theta_i}{dt_i} + T_{si} = T_{mi} \ (i = x, y, z) \tag{4. 8}$$

where I_i is the moment of inertia of the rotor, D_i is the viscous damping coefficie nt, Θ_i is the rotation angle of the rotor, T_{si} and T_{mi} are the friction torque and the torque acting on the rotor, respectively, and i is the rotation axis of the rotor.

4.2.1.2 Static torque characteristic analysis

Static torque characteristics analyses were conducted under the following four conditions. In addition to uniaxial motions, the characteristics of multi-axial motions were analyzed to see how a motion around one axis affects a motion around another. Fig. 4. 14 shows the position and the input current of the outer coils for tilting motions around the X- and Y-axes. Fig. 4. 15 shows the input current to the inner coils to rotate around the Z-axis. The 3-D finite element mesh model used in these analyses is shown in Fig. 2. 7, and Table 4. 2 shows the analysis conditions to compute the static torque characteristics.

The analyzed angular ranges of these analyses are from −40 to 40 degrees for a tilt motion and from 0 to 90 degrees for a rotation motion. Each coil is excited by a 2-A DC during tilt motion, and the inner coils are excited by 2-A 3-phase AC during rotation motion. In addition to the output torque characteristics, the cogging torque characteristics are also computed in each analysis (dashed lines in each figure). The results of the analyses are shown in Figs. 4. 17-22.

Table 4. 2. Analysis condition of static torque characteristics

Analyzed angle [degree]	−40 to 40	
Excitation current [A]	2 (DC)	
Number of excited coils	4	
Total CPU time [hour]	Tilt	14
	Rotation	16
Number of coil turns	600 (outer coils)	
	300 (inner coils)	

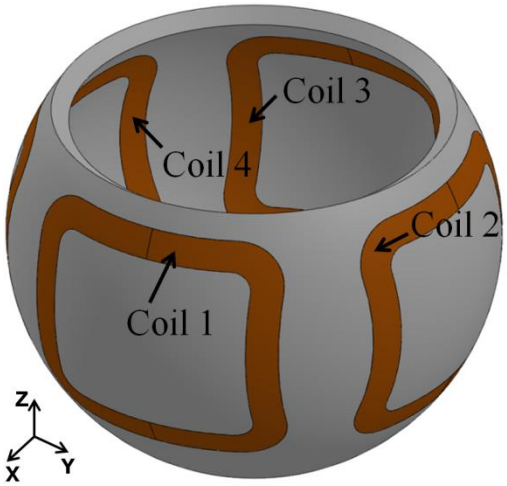

(a) Position of outer coils

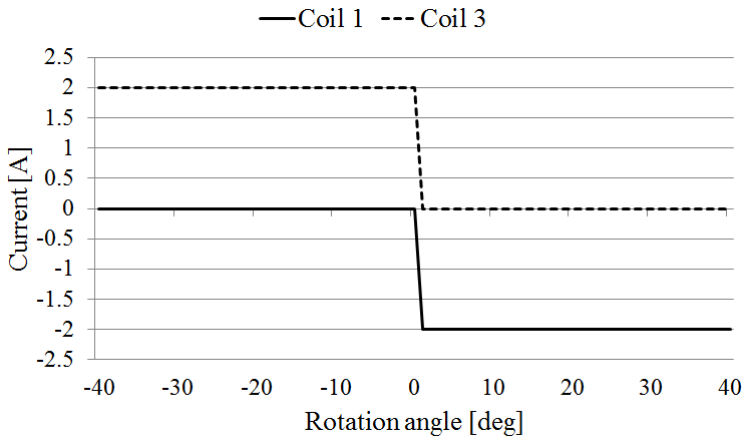

(b) Input current for tilting around X-axis

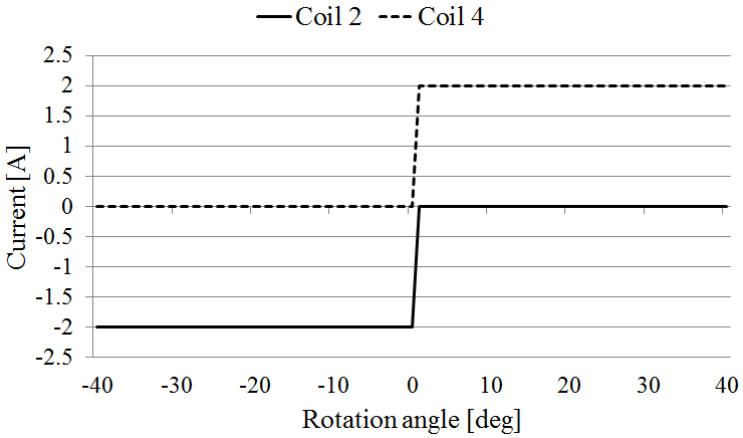

(c) Input current for tilting around Y-axis

Fig. 4.14. Input current to outer coils

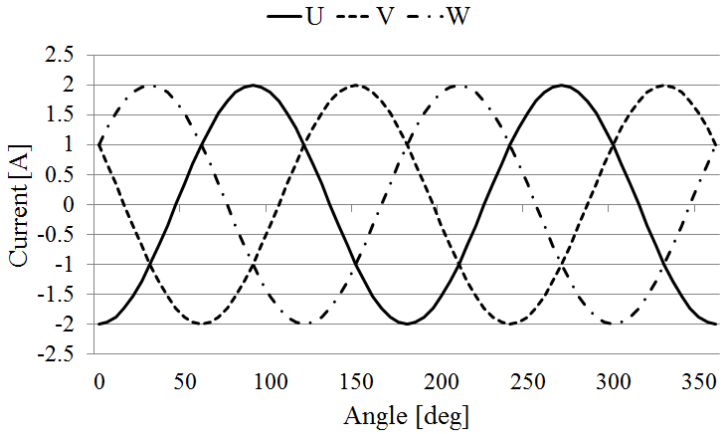

Fig. 4.15. Input current to inner coils for rotation around Z-axis

(a) Biaxial tilt motion

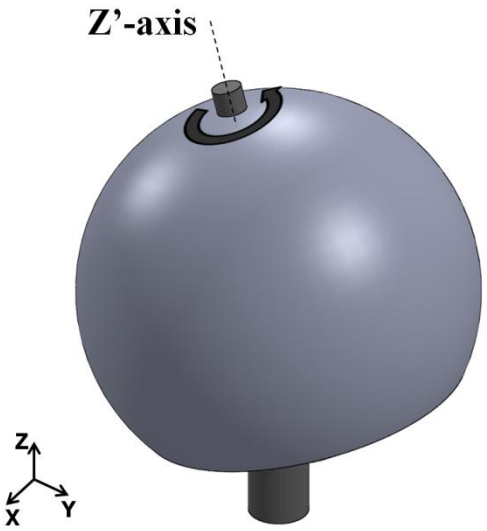

(b) Simultaneous rotation and tilt motion

Fig. 4. 16. Biaxial tilt motion and simultaneous rotation and tilt motion

4.2.1.2.1 Uniaxial tilt motion

From the result of the uniaxial tilt motion shown in Fig. 4. 17, it can be seen that the actuator is easily-controlled during tilt motion. Furthermore the cogging torque of this

actuator is relatively small and the equilibrium point is at the center since the cogging torque value is 0, and its gradient is negative when the actuator is tilted because the current density is decreased. The average output torque is 0.2 Nm.

4.2.1.2.2 Uniaxial rotation motion

Fig. 4. 18 shows the torque characteristics of the uniaxial rotation motion. The fundamental order of the cogging torque is 12, which is the least common multiple of the pole and slot numbers. The fundamental order of the excited torque is also 12 as shown in Fig. 4. 19. This means that the cogging torque is dominant in the excited torque ripple.

4.2.1.2.3 Biaxial tilt motion

The analyzed results shown in Fig. 4. 20 are the cogging and output torque characteristics of the biaxial tilt motion. In this analysis, the rotor tilts toward the 45 degrees angle due to the resultant force of the X- and Y-axes motions as shown in Fig. 4. 16 (a). Since all four coils on the stator are excited, the output torque is higher than that of uniaxial motion. Furthermore the cogging torque characteristics during biaxial tilt motion are about the same gradient as that during uniaxial tilt motion. Therefore the cogging torque characteristics will be the same during tilt motion in any arbitrary direction.

4.2.1.2.4 Simultaneous rotation and tilt motion

Figs. 4. 21 and 4. 22 are the analyzed results of the simultaneous rotation and tilt motion. Fig. 4. 16 (b) shows that the rotor was rotated around the Z'-axis which is the Z axis that has been rotated 20 degrees around the X-axis. From the analyzed result of the cogging torque, it can be seen that little cogging torque is generated around the

Y-axis since the rotor is tilted. This is the force that is trying to rotate the rotor back to its equilibrium position. As for the output torque, the Z'-axis torque is about 0.15 Nm, which is lower than that during uniaxial rotation motion. This is attributed to the decreased area of the coils in the inner stator that is facing the permanent magnets of the inner rotor.

The important information obtained from these results is that the output torque is always positive in all of the analyses. This shows that the actuator can rotate in the analyzed range. In addition to this, a notable characteristic is that the output torque around the X-axis during simultaneous rotation and tilt motion (solid line in Fig. 4. 22) is relatively flat and has little ripple. If there is a noticeable ripple, the current for a tilt motion must be adjusted constantly to maintain the tilt angle. Therefore, it can be deduced that simultaneous three degree of freedom control can be easily accomplished and the tilt motion and rotation motion can be controlled independently.

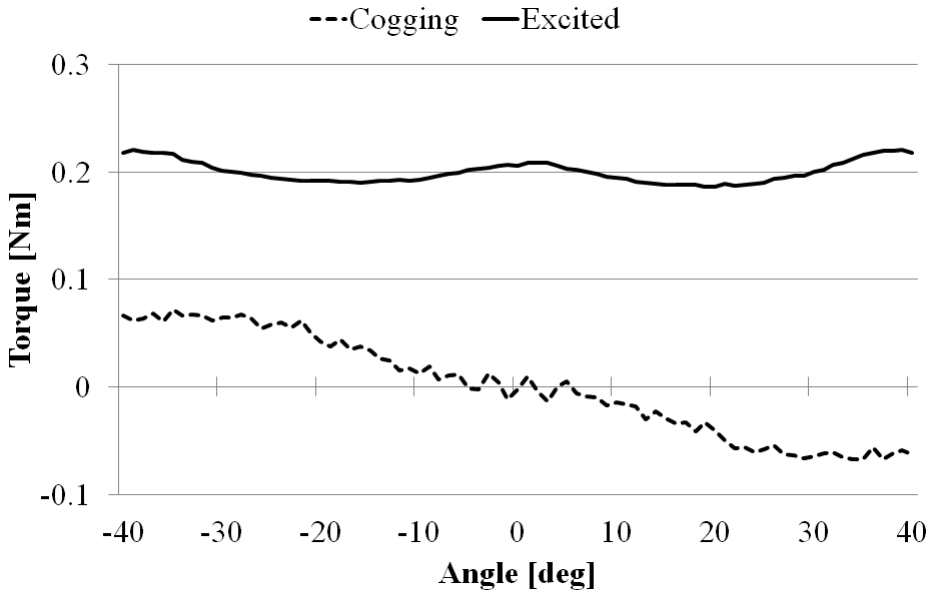

Fig. 4. 17. Torque characteristic of uniaxial tilt motion

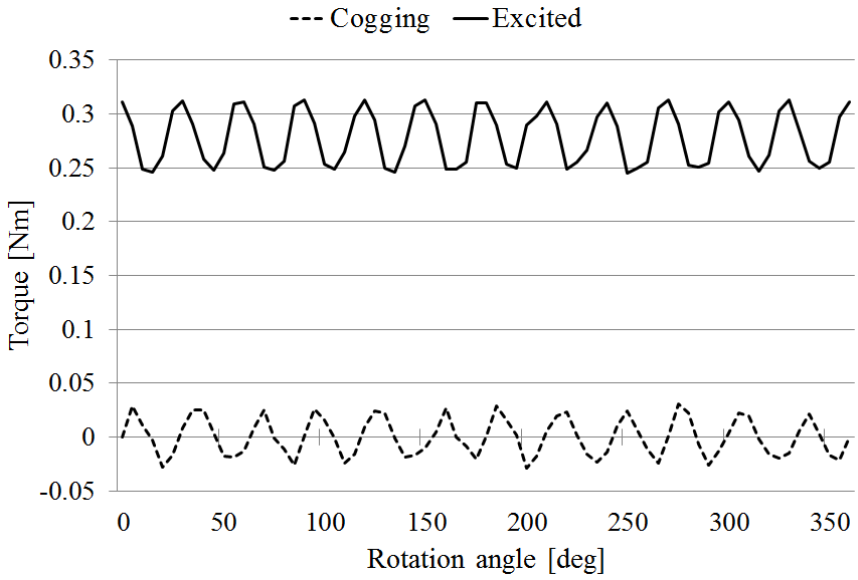

Fig. 4. 18. Torque characteristic of uniaxial rotation motion

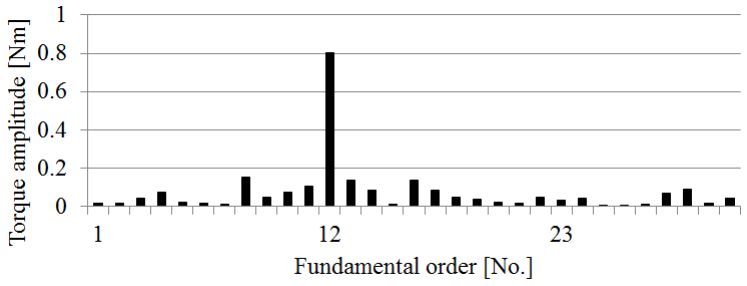

(a) FFT result of cogging torque waveform

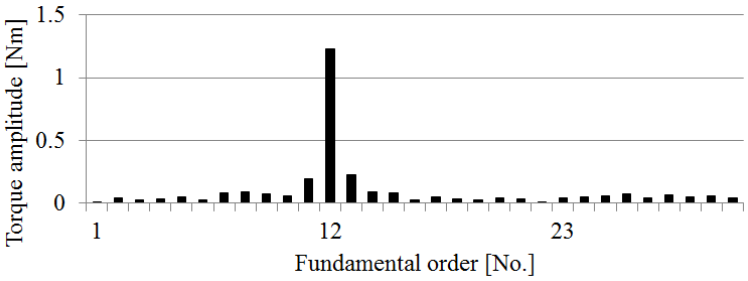

(b) FFT result of excited torque waveform

Fig. 4. 19. FFT results of uniaxial rotation motion

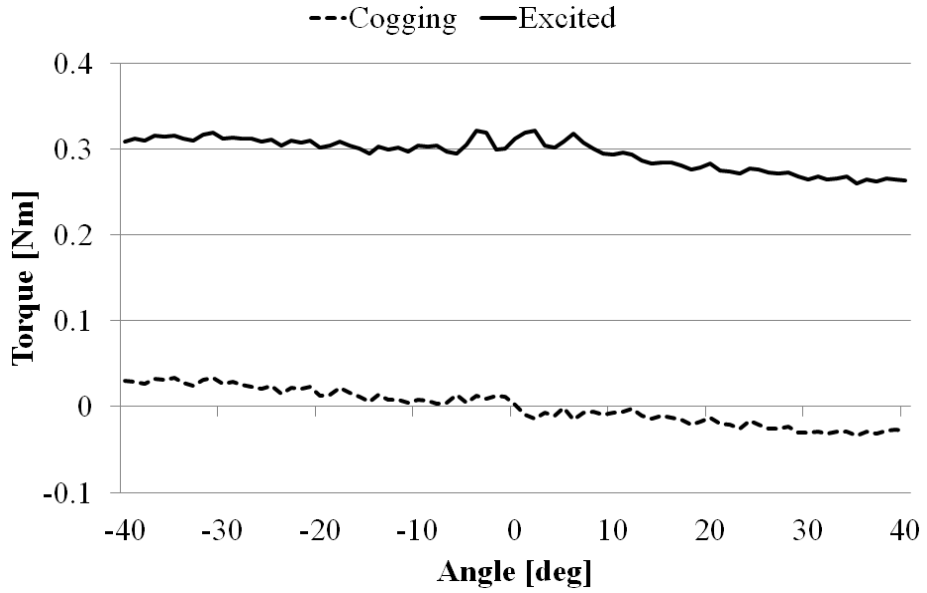

Fig. 4. 20. Torque characteristic of biaxial tilt motion

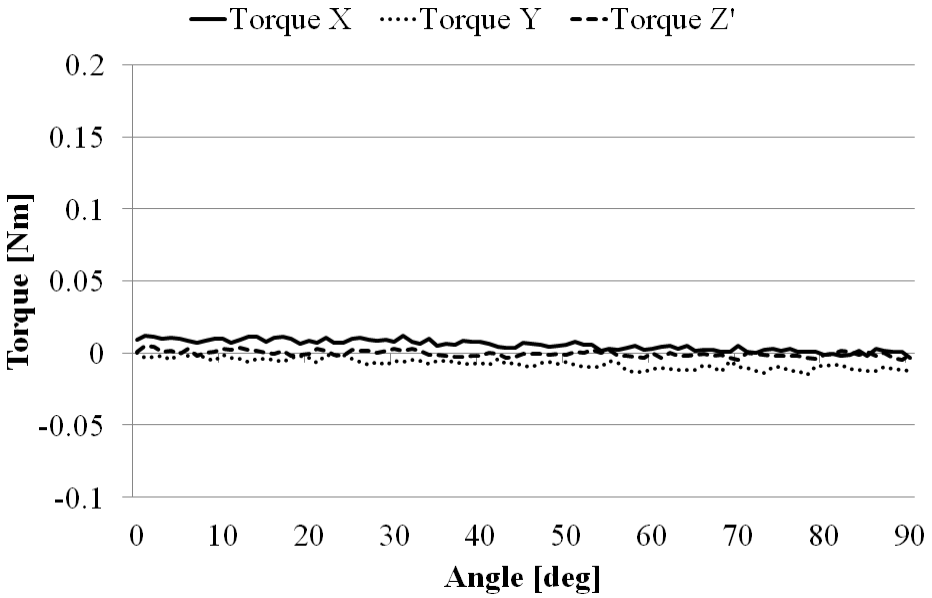

Fig. 4. 21. Cogging torque characteristic of simultaneous rotation and tilt motion

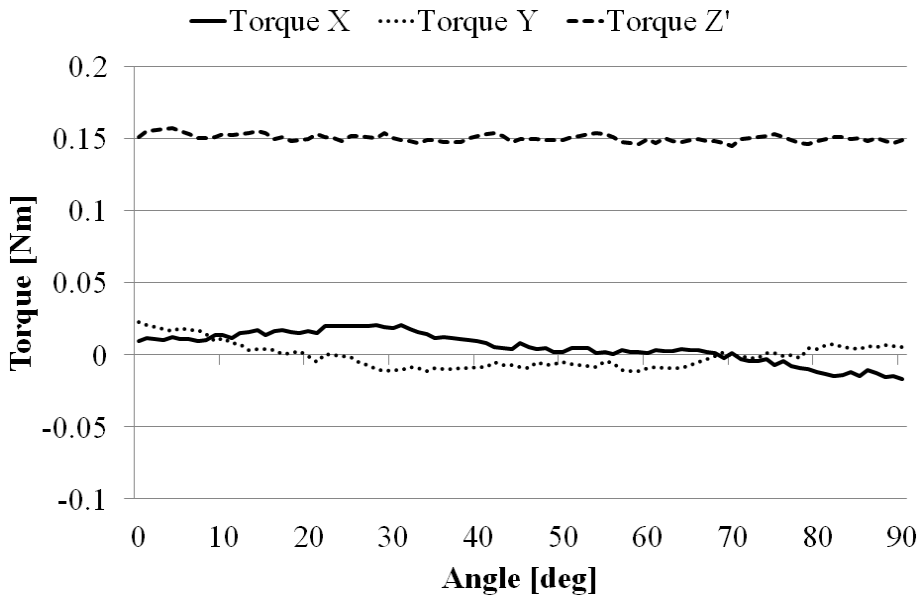

Fig. 4. 22. Excited torque characteristic of simultaneous rotation and tilt motion

4.2.1.3 Dynamic operating characteristic analysis

Dynamic operating characteristics analyses were conducted to confirm how the rotor behaves during each motion. The characteristics were computed under the following three conditions.

The 3-D finite element mesh model is the same as that used during the static torque analyses and Table 4. 3 shows the analysis conditions to compute the dynamic torque characteristics.

The outer coils are excited by a 2-A amplitude, 2-Hz frequency three-phase AC for rotation motions. The results of each characteristics analysis are shown in Figs. 4. 23 and 4. 25.

4.2.1.3.1 Uniaxial tilt motion

From the result of the uniaxial tilt motion shown in Fig. 4. 23, it can be seen that the rotor moves in a reciprocating motion. Though large initial transient amplitude, the rotor stabilizes subsequently.

4.2.1.3.2 Uniaxial rotation motion

In the rotation motion, the rotor should theoretically rotate 180 degrees per second because the frequency of the electrical angle is 2 Hz. As shown in Fig. 4. 24, the analyzed result shows a good agreement with this theoretical value and the rotor (mover) synchronizes with the rotating magnetic field, though small ripples which resulted mainly from the cogging torque can be seen.

4.2.1.3.3 Triaxial motion

Fig. 4. 25 shows the analyzed result of a triaxial simultaneous motion combining the circular motion and the tilted rotation. From the analyzed result, it can be confirmed that the rotor is rotating around the Z'-axis and at the same time the Z'-axis is rotating along a circular path. This result shows that a simultaneous triaxial motion is possible by just simply combing the current control for each uniaxial motion.

Table 4. 3. Analysis condition of dynamic characteristics

Number of element	738,768	
Number of time steps	Uniaxial rotation	80
	Other analyses	160
Total CPU time [hour]	Uniaxial rotation	14
	Other analyses	20
Moment of inertia [kg*m^2]	Tilt	1.62×10^{-4}
	Rotation	1.25×10^{-4}

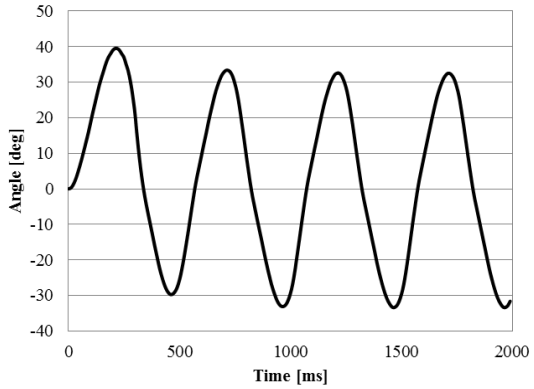

Fig. 4. 23. Operating characteristic of uniaxial tilt motion

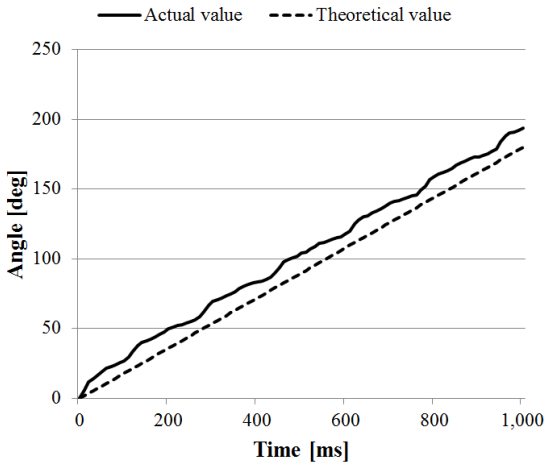

Fig. 4. 24. Operating characteristic of uniaxial rotation motion

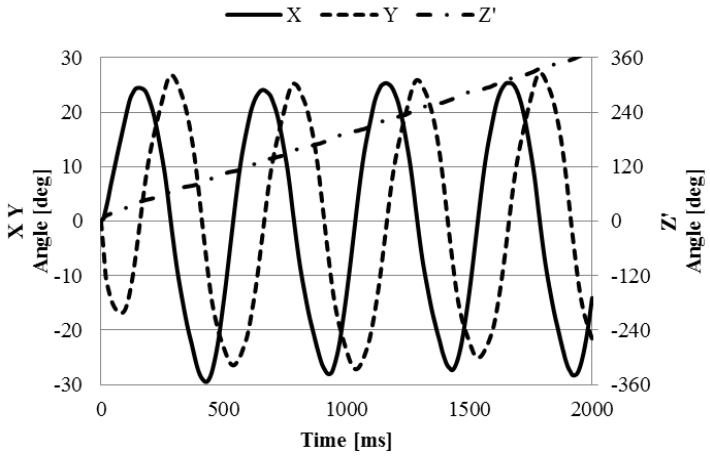

Fig. 4. 25. Operating characteristic of triaxial motion

4.2.2 Proposed controller scheme

The proposed ANFIS controller incorporates a fuzzy logic algorithm with a five-layer neural network structure. The output of the ANFIS controller is readjusted to reduce the error. A schematic diagram of the proposed ANFIS control of the system is shown in Fig. 4. 26. In this system, a modification signal is added into the input position before it is input into the position controller.

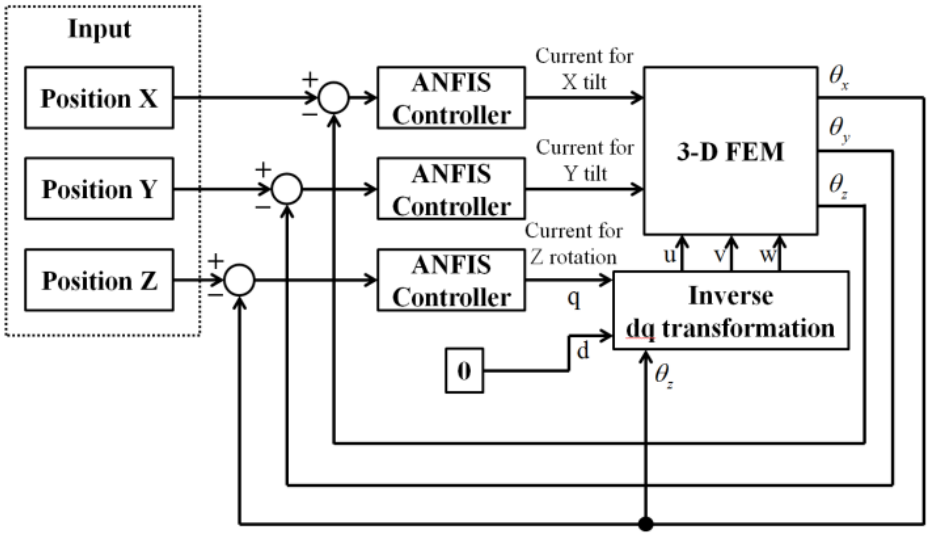

Fig. 4. 26. Block diagram of the proposed controller scheme

4.2.3 Analyzed results under feedback control

The analyzed result of the operating characteristics during tilt motion around the X-, Y- and Z-axes under PID control (P gain: 0.8, I gain: 0.04, D gain: 0.04) is shown in Fig. 4. 27, 29 and 31 where the position feedback system performs rather well, although small errors can be observed. The actual rotation angle under PID control has more smooth line like the shape of the desired angle. However, the actual angles are not accurate values.

The analyzed result of the operating characteristics during tilt motion around the X-,

Y- and Z-axes under ANFIS control is shown in Fig. 4. 28, 30 and 32 where the ANFIS control method is much more accurate and the error values between the desired and actual angles are smaller than that of the PID control.

These results also show that the position feedback control was successful around all axes, and that the proposed actuator can simultaneously rotate around 3 axes accurately with the control method.

The average errors when the PID and ANFIS control are used are shown in Table. 4. 4. The average errors under the PID and ANFIS control are about 1.4 degrees and about 0.6 degrees around X- and Y-axes. The average error around Z-axis is about 1.8 degrees (PID) and about 0.6 degrees (ANFIS).

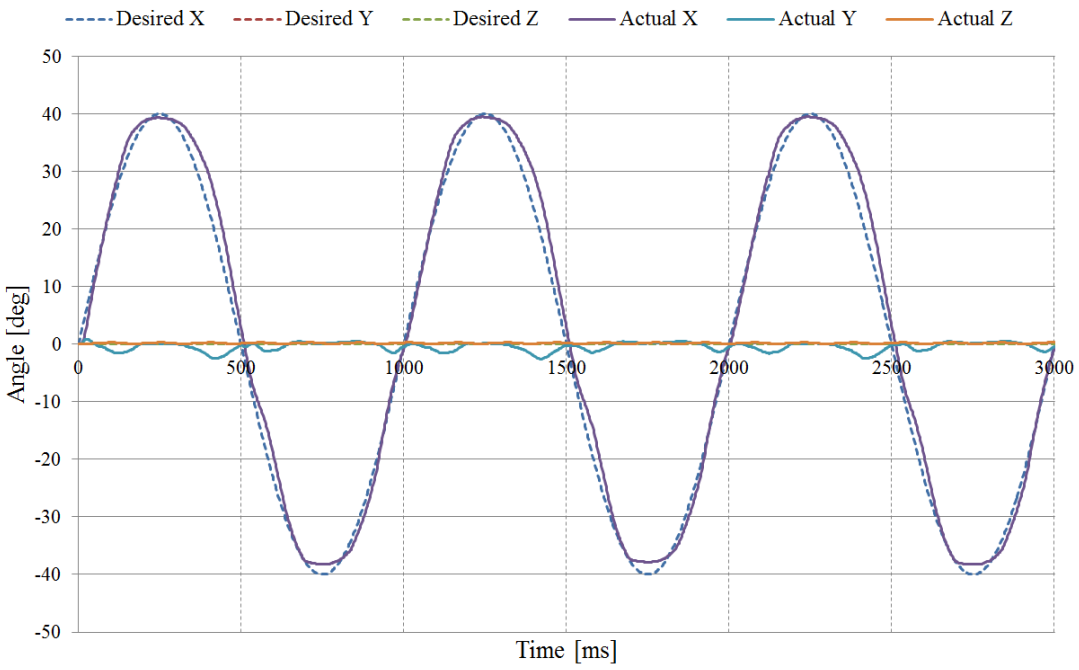

Fig. 4. 27. Result of the PID control, around X-axis

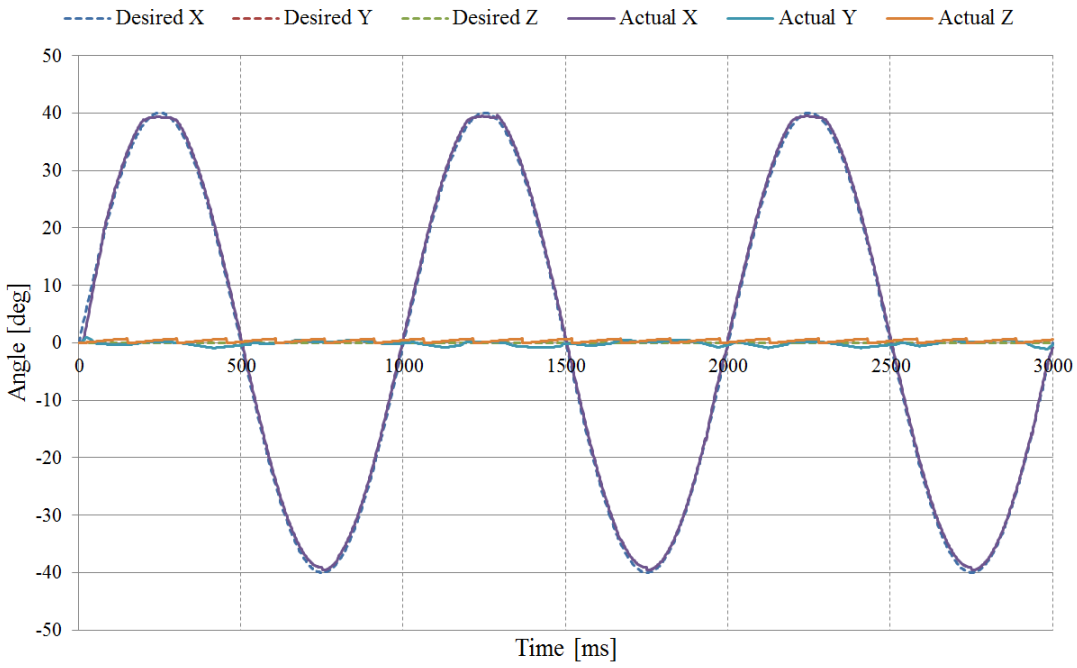

Fig. 4. 28. Result of the ANFIS control, around X-axis

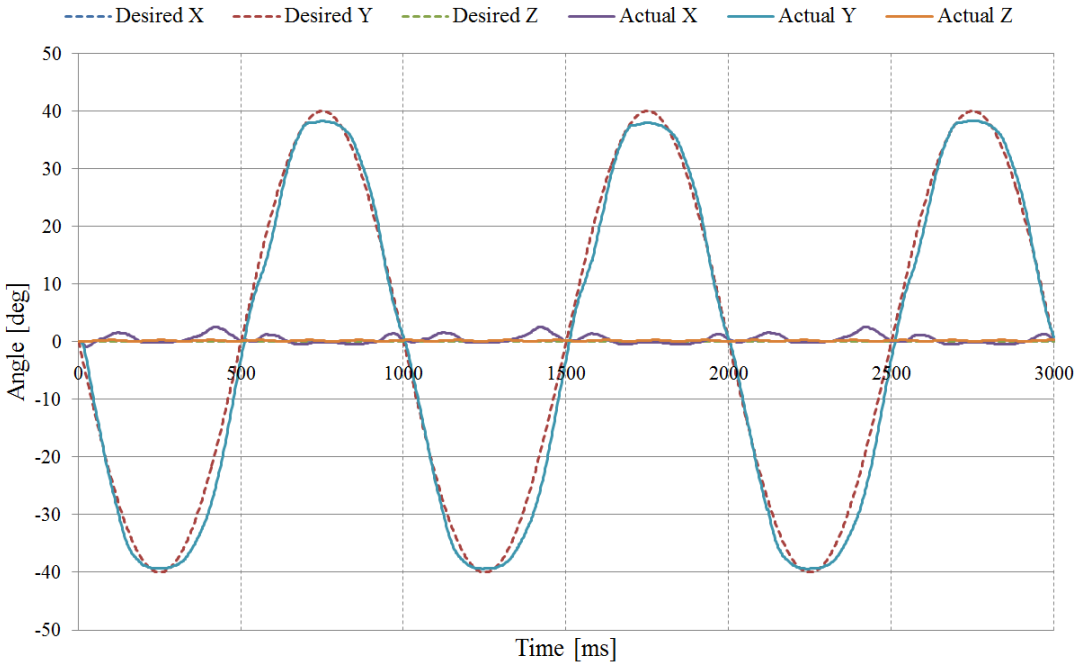

Fig. 4. 29. Result of the PID control, around Y-axis

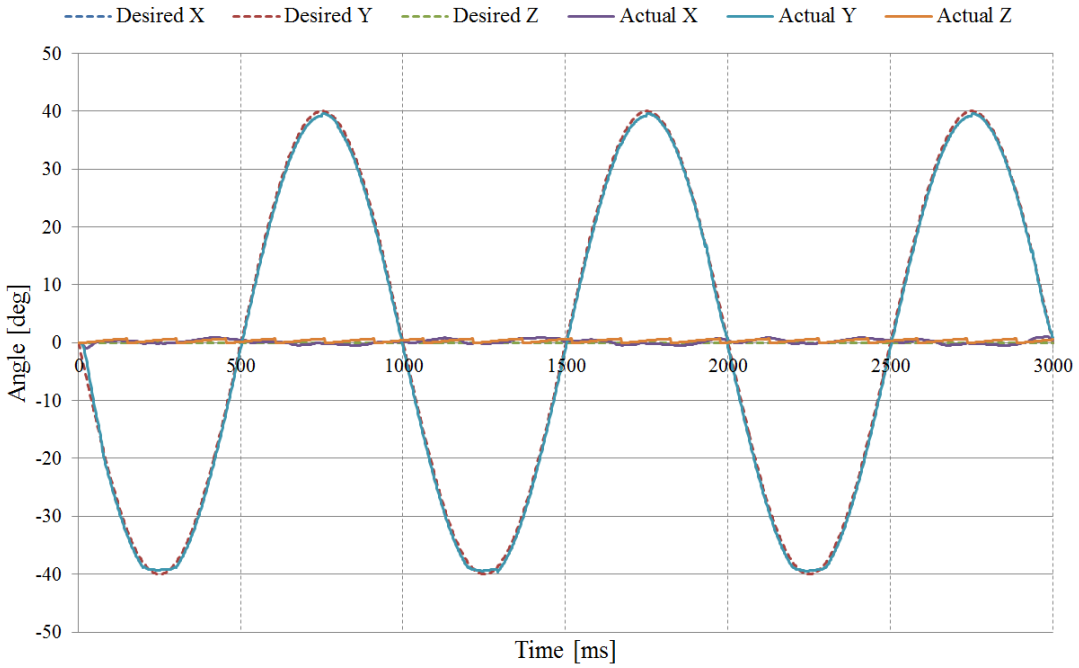

Fig. 4. 30. Result of the ANFIS control, around Y-axis

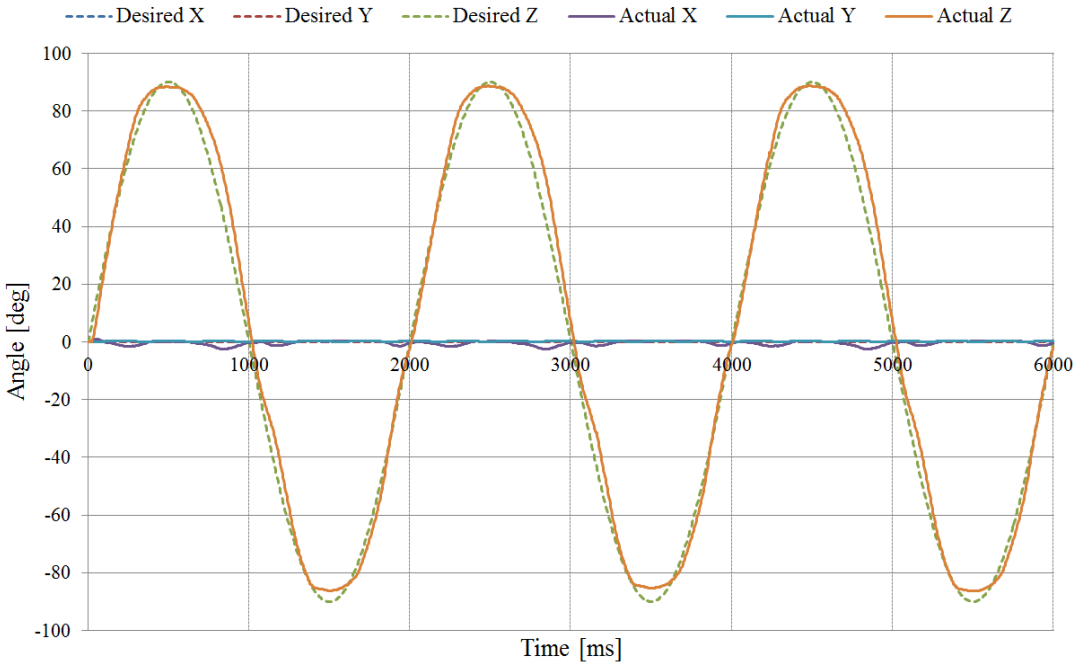

Fig. 4. 31. Result of the PID control, around Z-axis

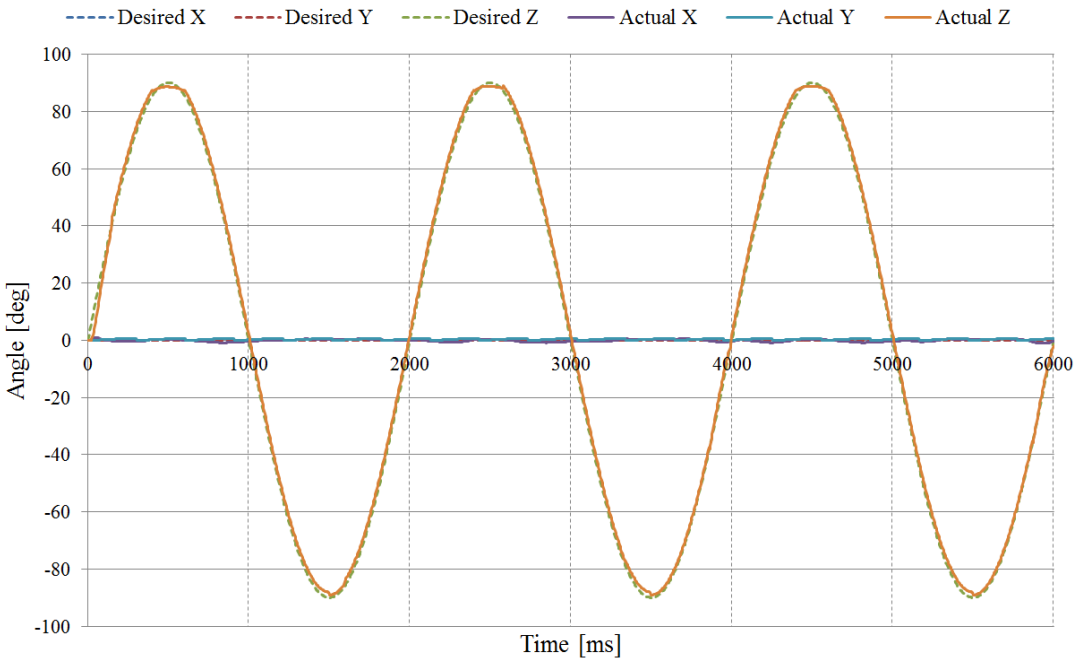

Fig. 4. 32. Result of the ANFIS control, around Z-axis

Table 4. 4. Average error of each control method

Control Method	Average error around X axis [degree]	Average error around Y axis [degree]	Average error around Z axis [degree]
PID control	1.42	1.42	1.8
ANFIS control	0.59	0.59	0.6

Chapter 5 Summary

This thesis extensively studied multi-degree-of-freedom spherical actuators and intelligent control.

Chapter 1 started off with the comparison of the conventional multi degree of freedom mechanism combining a spherical actuator and plurality of motors and clarified the advantage of the spherical actuator and the significance of a development. The previous research examples of a spherical actuator are showed. In addition, the purpose of this research, “Proposal of 3-degree-of-freedom spherical actuator using voice coil motor principle” and “Feedback control using adaptive neuro-fuzzy inference system (ANFIS) control method” are shown and the objective of the research is described.

Chapter 2 moved on to the topic of a new spherical actuator. In order to achieve a large angle of the tilt motion, high tilt torque, easy control and good dynamic performance, a design flow chart is considered. A proposed spherical actuator with a new structure is described. The structure of the proposed actuator and its operating principle are explained.

Chapter 3 explained the adaptive neuro fuzzy inference system (ANFIS) for feedback control of a spherical actuator.

In Chapter 4, the verification of a 2-DOF spherical actuator and proposed spherical actuator using ANFIS feedback control method are described. Firstly, in order to verify the ANFIS using a prototype of the 2-DOF spherical actuator. By the results of experiments, it became clear that the drive around each axis can be controlled without complicated inputs to each coil, which was required for the conventional spherical actuator. Secondly, the analyzed results of proposed spherical actuator with ANFIS

control. The analyzed results showed the feedback control method using ANFIS more accuracy than other control method.

The spherical actuator is capable of multi-DOF rotational motion within a single joint. Previous spherical actuators had problems with modeling, manufacturing and control. In this thesis, a novel spherical actuator with 3-DOF was proposed. In order to overcome the complex actuation principle of the existing spherical actuators, the proposed spherical actuator used the VCM principle.

The ANFIS is used for improving the performance of feedback control. ANFIS has the advantage of expert knowledge of the fuzzy inference system (FIS) and learning capabilities of the neural networks (NN) for control of a nonlinear system. The gains and parameters for feedback control are auto-tuned using a combination of the least squares estimation and back propagation. Therefore, a control method using ANFIS will produce more accurate results compared with other control methods.

References

1. J. Wang, K. Mitchell, G.W. Jewell, D. Howe, “Multi-degree-of-freedom spherical permanent magnet motors”, in: Robotics and Automation, 2001. Proceedings 2001 ICRA. IEEE International Conference on, vol. 2, pp. 1798-1805, 2001.
2. L. Yan, I.-M. Chen, C.K. Lim, G. Yang, K.-M. Lee, “Design, Modeling and Experiments of 3-DOF Electromagnetic Spherical Actuators, Springer, 2011.
3. M. K. Rashid, and Z. A. Khalil : “Configuration Design and Intelligent Stepping of a Spherical Motor in Robotic Joint”, Journal of Intelligent and Robotic Systems, Vol.40, pp.165-181, 2004.
4. L. Rossini, O. Ch'etelat, E. Onillon, and Y. Perriard : "Force and Torque Analytical Models of a Reaction Sphere Actuator Based on Spherical Harmonic Rotation and Decomposition," IEEE/ASME Transactions, Vol.PP, pp.1-13, 2012.
5. G.S. Chirikjian, D. Stein, “Kinematic design and commutation of a spherical stepper motor”, Mechatronics, IEEE/ASME Transactions on, 4, pp.342-353, 1999.
6. K. Davey, G. Vachtsevanos, R. Powers, “The analysis of fields and torques in spherical induction motors”, Magnetics, IEEE Transactions on, 23, pp. 273-282, 1987.
7. A. Foggia, E. Olivier, F. Chappuis, J.C. Sabonnadiere, “A new three degrees of freedom electromagnetic actuator”, in: Industry Applications Society Annual Meeting, 1988., Conference Record of the 1988 IEEE, vol. 1, pp. 137-141, 1988.
8. B. Dehez, G. Galary, D. Grenier, B. Raucent, “Development of a Spherical Induction Motor With Two Degrees of Freedom”, Magnetics, IEEE Transactions on, vol. 42, pp. 2077-2089, 2006.
9. K. –M. Lee, J. Pei, R. Roth, “Kinematic analysis of a three-degree-of-freedom

spherical wrist actuator", Mechatronics, pp. 581-605, 1994.

10. Zhi Zhou, Kok-Meng Lee, "Real-time motion control of a multi-degree-of-freedom variable reluctance", in: Robotics and Automation, 1996. Proceedings., 1996 IEEE International Conference on, vol. 3, pp. 1050-4729, 1996.
11. Kok-Meng Lee, Zhiyong Wei, Jeffry Joni, "Parametric study on pole geometry and thermal effects of a VRSM", in: Robotics, Automation and Mechatronics, 2004 IEEE Conference on, vol. 1, pp. 548-553, 2004.
12. Kok-Meng Lee, Hungsun Son, "Torque Model for Design and Control of a Spherical Wheel Motor", in: Advanced Intelligent Mechatronics. Proceedings, 2005 IEEE/ASME International Conference on, pp. 335-340, 2005.
13. Kok-Meng Lee, Hungsun Son, J. Joni, "Concept Development and Design of a Spherical Wheel Motor (SWM)", Proceedings of the 2005 IEEE International Conference on Robotics and Automation, pp. 3652-3657, 2005.
14. Liang Yan, I-Ming Chen, Chee Kian Lim, Guilin Yang, Wei Lin, Kok-Meng Lee, "Design and Analysis of a Permanent Magnet Spherical Actuator", IEEE/ASME Transactions on Mechatronics, vol. 13, pp. 239-248, 2008.
15. Yusuf Öner, " A permanent magnet spherical rotor design and three dimensional static magnetic analysis", Sensors and Actuators A: Physical, vol. 137, pp. 200-208, 2007.
16. T. Shigeki, Z. Guoqiang, M. Osamu, "Development of new generation spherical ultrasonic motor", Proceedings of IEEE International Conference on Robotics and Automation, vol. 3, pp. 2871-2876, 1996.
17. E. Purwanto, S. Toyama, "Control method of a spherical ultrasonic motor", Proceedings 2003 IEEE/ASME International Conference on Advanced Intelligent Mechatronics (AIM 2003), vol. 2, pp. 1321-1326, 2003.
18. Chunsheng Zhao, Zhirong Li, Weiqing Huang, "Optimal design of the stator of a three-DOF ultrasonic motor", vol. 121, pp. 494-499, 2005.
19. T. Takizawa, M. Shinoda, K. Wakabayashi, K. Takamine, Y. Ikawa, I. Satoh, "High Speed Access Mechanism For 90mm 1 "Height Optical Disk Drive", Conference

Digest Joint International Symposium on Optical Memory and Optical Data Storage 1993, pp. 93-94, 1993.

20. Chang Seop Koh, Osama A. Mohammed, Jun-O Kim, Song-yop Hahn, “Optimum design of voice coil motor with constant torque coefficients using evolution strategy”, vol. 75, pp. 6045-6047, 1994.
21. Dong-Ju Lee, Kang-Nyung Lee, No-Cheol Park, Young-Pil Park, Hyuk Kim, Suk-Won Lee, Hyoung Gil Choi, Moon Gu Lee, Jiho Uh, Jung-Woo Park, Yong-Hwan Choi, Dong-Jin Lee, “Development of 3-axis nano stage for precision positioning in lithography”, IEEE International Conference Mechatronics and Automation, 2005, vol. 3, pp. 1598-1603, 2005.
22. F. C. Williams, E. R. Laithwaite, J. F. Eastham, “Development and design of spherical induction motors”, Proceedings of the IEE – Part A: Power Engineering, vol. 106, pp. 471-484, 1959.
23. DM Munnoz, “Spherical Machines: A Literature Review [Elektronisk resurs], IEA, 2005.
24. Shigeki Toyama, A. Kobayashi, “Development of Spherical Ultrasonic Motor”, CIRP Annals – Manufacturing Technology, vol. 45, pp. 27-30, 1996.
25. Tomoaki Mashimo, Shigeki Toyama, Hiroshi Ishida, “Design and implementation of spherical ultrasonic motor”, IEEE Transactions on Ultrasonics, Ferroelectrics, and Frequency Control, vol. 56, pp. 2514-2521, 2009.
26. W. Wang, K. Wang, G. W. Jewell, D. Howe, “Design and control of a novel spherical permanent magnet actuator with three degrees of freedom”, IEEE/ASME Transactions on Mechatronics, vol. 8, pp. 457-468, 2003.
27. B. Ackermann, H. Steinbusch, T. Vollmer, J. Wang, G. W. Jewell, D. Howe, “A spherical permanent magnet actuator for a high-fidelity force-feedback joystick”, Mechatronics, vol. 14, pp. 327-339, 2004.
28. Hungsun Son, Kok-Meng Lee, “Distributed Multipole Models for Design and Control of PM Actuators and Sensors”, IEEE/ASME Transactions on Mechatronics, vol. 13, pp. 228-238, 2008.

29. Kok-Meng Lee, Kun Bai, Jungyoul Lim, “Dipole Models for Forward/Inverse Torque Computation of a Spherical Motor”, IEEE/ASME Transactions on Mechatronics, vol. 14, pp. 46-54, 2009.
30. Hungson Son, Kok-Meng Lee, “Open-Loop Controller Design and Dynamic Characteristics of a Spherical Wheel Motor”, IEEE Transactions on Industrial Electronics, vol. 57, pp. 3475-3482, 2010.
31. Liang Yan, I-Ming Chen, Chee Kian Lim, Guilin Yang, Kok-Meng Lee, “Modeling and Iron-Effect Analysis on Magnetic Field and Torque Output of Electromagnetic Spherical Actuators With Iron Stator”, IEEE/ASME Transactions on Mechatronics, vol. 17, pp. 1080-1087, 2012.
32. J. Wang, G. W. Jewell, D. Howe, “Modelling of a novel spherical permanent magnet actuator”, Proceedings of International Conference on Robotics and Automation, vol. 2, pp. 1190-1195, 1997.
33. K. H. Ang, G. Chong, and Y. Li, “PID control system analysis, design, and technology,” IEEE Trans. Control Syst. Technol., vol. 13, no. 4, pp. 559-576, 2005.
34. J.-S.R. Jang, “ANFIS: Adaptive-network-based fuzzy inference system,” IEEE Transactions on Systems, Man, and Cybernetics, vol. 23, pp. 665-685, 1993.
35. Chun-Tian Cheng, Jian-Yi Lin, Ying-Cuang Sun, Kwokwing Chau, “Long-Term Prediction of Discharges in Manwan Hydropower Using Adaptive-Network-Based Fuzzy Inference Systems Models,” ICNC 2005, pp. 1152-1161, 2005.
36. Simon Haykin, “Neural Networks and Learning Machines,” Prentice Hall, 2008.
37. Warren S. McCulloch and Walter H. Pitts, “A Logical Calculus of The Ideas Immanent in Nervous Activity,” Bull Math Biophys, vol. 5, pp. 115-133, 1943.
38. W. Duch, N. Jankowski, “Survey of neural transfer function,” Neural computing surveys 2, pp. 163-212, 1999.
39. A.K. Jain, M. Jianchang, K.M. Mohiuddin, “Artificial neural networks: a tutorial,” Computer 29 (3), pp. 1-44, 1996.
40. H. Takagi, “Fusion technology of neural networks and fuzzy systems: a chronicled progression from the laboratory to our daily lives,” International Journal of

Applied Mathematics and Computer Science, Vol. 10, pp. 647-673, 2000.

41. B. Widrow, M. E. Hoff, “Adaptive switching circuits,” IRE WESCON Convention Record, pp. 96-104, 1960.
42. T. Takagi and M. Sugeno, “Derivation of fuzzy control rules from human operator’s control actions,” in Proceedings IFAC Symposium Fuzzy Information, Knowledge Representation and Decision Analysis, pp. 55-60, 1983.
43. R.J.S. Jang, C.T. Sun, and E. Mitzutani, “Neuro-Fuzzy and Soft Computing,” A Computational Approach to Learning and Machine Intelligence, Prentice-Hall, Inc, 1997.

Research Achievements

Published Papers

(1) J. Chu, N. Niguchi, K. Hirata, "Hybrid Artificial Intelligent Control for Feedback Control of Outer Rotor Spherical Actuator", Sensing Technology: Current Status and Future Trends IV, Journal of SPRINGER, Vol. 12, pp.253-268, 2015.01

(2) Junghyun Chu, Noboru Niguchi, Katsuhiro Hirata, "Analysis of a 3-Degree-of-Freedom Spherical Actuator using VCM principle", The transactions of the Korean Institute of Power Electronics, 2017.06

International Conferences

(1) Junghyun Chu, Noboru Niguchi, Katsuhiro Hirata, "Feedback Control of Outer Rotor Spherical Actuator Using Adaptive Neuro-Fuzzy Inference System", Proceedings of the Seventh International Conference on Sensing Technology, Wellington, S7.20, pp. 405-409, 2013.12.

(2) J. Chu, N. Niguchi, K. Hirata, "Design and analysis of a new spherical actuator," Proceedings of IEEE International Magnetics Conference (Intermag2015), Beijing, China, BG-11, 2015.05.